

1 **Modelling the climatic drivers determining photosynthesis and carbon allocation**  
2 **in evergreen Mediterranean forests using multiproxy long time series**

3 <sup>1,\*</sup>Gea-Izquierdo G, <sup>2</sup>Guibal F, <sup>3</sup>Joffre R, <sup>3</sup>Ourcival JM, <sup>4</sup>Simioni G, <sup>1</sup>Guiot J

4 <sup>1</sup>CEREGE UMR 7330, CNRS/Aix-Marseille Université. Europole de l'Arbois BP 80  
5 13545 Aix-en-Provence cedex 4, France. <sup>2</sup>IMBE, CNRS /Aix-Marseille Université  
6 UMR 7263 Europole de l'Arbois BP 8013545 Aix-en-Provence cedex 4, France. <sup>3</sup>Centre  
7 d'Ecologie Fonctionnelle et Evolutive CEFE, UMR 5175, CNRS - Université de  
8 Montpellier - Université Paul-Valéry Montpellier – EPHE, 1919 Route de Mende,  
9 34293 Montpellier Cedex 5, FRANCE. <sup>4</sup>Ecologie des Forêts Méditerranéennes, INRA  
10 UR 629, Domaine Saint Paul, 84914 Avignon Cedex 9, France.

11 \* Author for correspondence: [gea-izquierdo@cerege.fr](mailto:gea-izquierdo@cerege.fr)

12  
13 **Abstract**

14 Climatic drivers limit several important physiological processes involved in  
15 ecosystem carbon dynamics including gross primary productivity (GPP) and carbon  
16 allocation in vegetation. Climatic variability limits these two processes differently. We  
17 developed an existing mechanistic model to analyse photosynthesis and variability in  
18 carbon allocation in two evergreen species at two Mediterranean forests. The model was  
19 calibrated using a combination of eddy covariance CO<sub>2</sub> flux data, dendrochronological  
20 time series of secondary growth and forest inventory data. The model was modified to  
21 be climate explicit in the key processes addressing acclimation of photosynthesis and  
22 the pattern of C allocation, particularly to water stress. It succeeded to fit both the high-  
23 and the low-frequency response of stand GPP and carbon allocation to stem growth.  
24 This would support its capability to address both C-source and C-sink limitations.  
25 Simulations suggest a decrease in mean stomatal conductance in response to recent

26 enhancement in water stress and an increase in mean annual intrinsic water use  
27 efficiency (iWUE) in both species during the last 50 years. However, this was not  
28 translated into a parallel increase in ecosystem water use efficiency (WUE). Interannual  
29 variability of WUE followed closely that of iWUE at both sites. Nevertheless, long-term  
30 decadal variability of WUE followed the long-term decrease in annual GPP matching  
31 the local trend in annual precipitation observed since the 1970s at one site. In contrast,  
32 at the site where long-term precipitation remained stable GPP and WUE did not show a  
33 negative trend and the trees buffered the climatic variability. In our simulations these  
34 temporal changes would be related to acclimation processes to climate at the canopy  
35 level including modifications in LAI and stomatal conductance, but also partly related  
36 to increasing [CO<sub>2</sub>] because the model includes biochemical equations where  
37 photosynthesis is directly linked to [CO<sub>2</sub>]. Long-term trends in GPP did not match those  
38 in growth, in agreement with the C-sink hypothesis. There is a great potential to use the  
39 model with abundant dendrochronological data and analyse forest performance under  
40 climate change. This would help to understand how different interfering environmental  
41 factors produce instability in the pattern of carbon allocation, hence the climatic signal  
42 expressed in tree-rings.

43

44 **Keywords:** *Pinus halepensis*, *Quercus ilex*, process-based model, dendrochronology,  
45 eddy covariance; global change.

## Introduction

46

47 Global change challenges forest performance because it can enhance forest  
48 vulnerability (IPCC 2013). Trees modify multiple mechanisms at different scales to  
49 tackle with environmental stress, including changes in photosynthesis and carbon  
50 allocation within plants (Breda et al. 2006; Niinemets 2007; Chen et al. 2013). Many  
51 factors affect the different physiological processes driving forest performance. Among  
52 them, the net effect of rising CO<sub>2</sub> mixing ratio ([CO<sub>2</sub>]) and climate change is  
53 meaningful to determine the forests' capacity of acclimation to enhanced xericity  
54 (Peñuelas et al. 2011; Keenan et al. 2011; Fatichi et al. 2014). Forest process-based  
55 models have been developed to mimic these mechanisms. They can include different  
56 levels of complexity but generally implement calculations of leaf photosynthesis up-  
57 scaled to the canopy and carbon allocated to different plant compartments (Le Roux et  
58 al. 2001; Schaefer et al. 2012; De Kauwe et al. 2013). Although there is evidence that  
59 the tree performance depends to some extent on stored carbohydrates (Breda et al. 2006;  
60 McDowell et al. 2013; Dickman et al. 2014), these models have received some criticism  
61 when used to understand plant performance in response to climate change. This is in  
62 part because they are C-source oriented, therefore can exhibit certain limitations to  
63 represent the C-sink hypothesis (i.e. that growth rates are limited by environmental  
64 factors such as water stress, minimum temperature or nutrient availability rather than by  
65 carbohydrate availability) and address dysfunctions related to the tree hydraulics  
66 (Millard et al. 2007; Breshears et al. 2009; Sala et al 2012; Körner et al. 2013;  
67 McDowell et al. 2013; Fatichi et al. 2014).

68 Complex process-based models profit from multiproxy calibration, particularly  
69 when such data are applied at different spatio-temporal scales (Peng et al. 2011). The  
70 temporal scale can be approached using time growth series of dendrochronological data.

71 However the analysis of the past always adds uncertainties related to the influence of  
72 unknown stand conditions to properly scale productivity. Flux data including stand  
73 productivity can be estimated using the eddy covariance technique (Baldocchi 2003).  
74 These data overcome many of the limitations of dendroecological data (e.g. intra-annual  
75 resolution, control of stand conditions and scaling of net productivity) but they lack  
76 their spatial and temporal coverage. Thus, CO<sub>2</sub> flux data can be used to implement  
77 unbiased models of canopy photosynthesis, and then combined with dendroecological  
78 data to study how carbon is allocated to stem growth as a function of environmental  
79 forcing (Friedlingstein et al. 1999; Chen et al. 2013, McMurtrie & Dewar 2013).

80 Mechanistic models can be also used to analyse the environmental factors  
81 determining instability in the climate-growth response (D'Arrigo et al. 2008). Different  
82 process-based models have been applied with dendroecological data used either in  
83 forward or inverse mode (see Guiot et al. 2014 for a review). Among these models, the  
84 process-based model MAIDEN (Misson 2004) was originally developed using  
85 dendroecological data. The model explicitly includes [CO<sub>2</sub>] to calculate photosynthesis  
86 (hence its influence on carbon allocation) and includes a carbohydrate storage reservoir.  
87 The latter being one of its strengths compared to other models (Vaganov et al. 2006;  
88 Sala et al. 2012; Guiot et al. 2014). It has been previously employed to analyse growth  
89 variability in one temperate and two Mediterranean species (Misson et al. 2004;  
90 Gaucherel et al. 2008) and recently on inverse mode (also including C and O stable  
91 isotopes) to reconstruct past climate (Boucher et al. 2014). However, it requires further  
92 development to ensure that it provides unbiased estimates of forest productivity and  
93 assesses uncertainties in the response of trees to climatic variability at a greater spatial  
94 scale at the regional level. Particularly, its parameterization would need improvement if



95 the model is applied to assess how climate modulates forest performance and the pattern  
96 of C allocation within plants (Niinemets & Valladares 2004; Fatichi et al. 2014).

97 In this study we use multiproxy data to develop a process-based model and  
98 investigate how evergreen Mediterranean forests have modified stand photosynthesis  
99 and carbon allocation in response to interacting climatic factors and enhanced [CO<sub>2</sub>] in  
100 the recent past. The first objective was to develop a process-based model based on  
101 MAIDEN (Misson 2004). Within the new version of the model, photosynthesis, carbon  
102 allocation, canopy turnover and phenology are now calculated using climate explicit  
103 functions with a mechanistic basis. The model is adapted to give unbiased estimates of  
104 canopy photosynthesis and stem growth using instrumental data. Specifically, within the  
105 new model formulation: (1) photosynthesis is penalized by prolonged water stress  
106 conditions through reductions in leaf area index (LAI) and maximum photosynthetic  
107 capacity; (2) the pattern of carbon allocation is directly determined by soil water content  
108 (i.e. water stress) and temperature through nonlinear relationships; (3) these  
109 relationships can be contrasting for different phenophases and affect independently  
110 photosynthesis and the pattern of C allocation. Once the model was developed, a second  
111 objective was to analyse how [CO<sub>2</sub>] and climatic variability affect the temporal  
112 instability in annual forest productivity, water use efficiency and carbon allocation. We  
113 hypothesise that they will exhibit differences in their long-term variability in relation to  
114 recent climate change driven by different functional acclimation processes within trees.

115

## 116 **Material and methods**

### 117 *Study sites and climatic data*

118 The study sites were two evergreen Mediterranean monitored forests in Southern  
119 France where CO<sub>2</sub>, water vapour and energy fluxes are measured using the Eddy

120 covariance technique (Baldocchi 2003). Both sites are included in FLUXNET  
121 (<http://fluxnet.ornl.gov/>). The first site Fontblanche (43.2° N, 5.7° E, 420 m) is a mixed  
122 stand where *Pinus halepensis* Mill. dominates the open top canopy layer reaching about  
123 12 m, *Quercus ilex* L. forms a lower canopy layer reaching about 6 m and there is a  
124 sparse shrub understory including *Quercus coccifera* L. (Simioni et al. 2013). The  
125 second site, Puechabon (43.4°N, 3.4° E, 270 m), is a dense coppice in which overstory is  
126 dominated by *Q. ilex* with density around 6,000 stems/ha (Rambal et al. 2004; Limousin  
127 et al. 2012). Both forests grow on rocky and shallow soils with low retention capacity  
128 and of Jurassic limestone origin. The climate is Mediterranean, with a water stress  
129 period in summer, cold or mild winters and most precipitation occurring between  
130 September and May. Meteorological data were obtained from the neighbouring stations  
131 of St. Martin de Londres (for Puechabon) and Aubagne (for Fontblanche). According to  
132 those data Puechabon is colder and receives more precipitation than Fontblanche (Table  
133 1). Meteorological data showed a decrease in total rainfall since the 1960s in Puechabon  
134 but no trend in Fontblanche. Both sites exhibit a positive trend in temperatures more  
135 evident for the maximum values (Figure A1).

136 We assumed that GPP is driven by the top pine and/or oak layers and that the  
137 percentage of LAI related to the understory shrub layer will behave like that of the oak  
138 species (evergreen, shrubby). For Fontblanche we considered a maximum leaf area  
139 index ( $LAI_{max}$ ) of  $2.2 \text{ m}^2 \cdot \text{m}^{-2}$  ( $3 \text{ m}^2 \cdot \text{m}^{-2}$  plant area index, PAI), composed by a 70% of  
140 pine and 30% of oak (Simioni et al. 2013). For Puechabon we considered a  $LAI_{max}$  of  
141  $2.0 \text{ m}^2 \cdot \text{m}^{-2}$  ( $2.8 \text{ m}^2 \cdot \text{m}^{-2}$  PAI) monospecific of *Q. ilex* (Baldocchi et al. 2010; Limousin et  
142 al. 2012). Specific leaf area ( $SLA$ ) considered was  $0.0045 \text{ m}^2 \cdot \text{g}^{-1}$  for *Q. ilex* and  $0.0037$   
143  $\text{m}^2 \cdot \text{g}^{-1}$  for *P. halepensis*, respectively (Hoff & Rambal 2003; Maseyk et al. 2008).

144

145 *The model*

146 We used MAIDEN (Misson 2004), a stand productivity mechanistic model driven  
147 by a number of functions and parameters representing different processes. The model  
148 inputs are precipitation, maximum and minimum temperature and CO<sub>2</sub> with a daily time  
149 step. This model has been previously implemented for monospecific forests including  
150 two oaks and one pine species using dendroecological chronologies of growth and,  
151 when available, stand transpiration estimates from sap-flow sensors (Misson et al. 2004;  
152 Gaucherel et al. 2008). However, the model has never been compared to actual CO<sub>2</sub>  
153 data to ensure that it provides unbiased estimates of forest productivity. In this study,  
154 the model was further developed to match ground-based observations and generalize  
155 model use by modifying the photosynthesis and allocation modules (including the  
156 different phenophases) in relation to climatic drivers. To properly scale model outputs  
157 and get unbiased estimates of stand productivity we used CO<sub>2</sub> eddy covariance fluxes  
158 (Baldocchi 2003). Different parameters were calibrated to different data sources,  
159 including some species-dependent and some site-dependent parameters, as follows. The  
160 transpiration rate (E) of day *i* is calculated using a conductance approach as  
161  $E(i) = g_s(i) \cdot VPD(i) / P_{atm}(i)$ , where  $P_{atm}$  is atmospheric pressure and  $g_s$  and  $VPD$  are  
162 stomatal conductance and vapour pressure deficit, respectively, as described below  
163 (Misson 2004). Those other equations used to calculate micrometeorological  
164 covariates, soil humidity and photosynthetic active radiation, as well as those functions  
165 describing the water cycle (including soil evaporation and plant transpiration) are  
166 explained in the original model formulation from Misson (2004). Therefore they won't  
167 be described here. The rest of the model was modified as follows.

168

169 *Modelling the effect of climatic forcing on photosynthesis*

170 Leaf photosynthesis ( $A_n$ ) is calculated based on the biochemical model of Farquhar  
 171 et al. (1980).  $A_n$  is a function of the carboxylation ( $V_c$ ), oxygenation ( $V_o$ ) and dark  
 172 respiration rates ( $R_d$ ):  $A_n(i) = V_c - 0.5V_o - R_d$ ; where photosynthesis at day  $i$  is limited by  
 173 either the rate of carboxylation when Rubisco is saturated ( $W_c$ ) or when it is limited by  
 174 electron transport ( $W_j$ ), i.e.  $A_c = V_c - 0.5V_o = \min\{W_c, W_j\}$ .  $R_d$  was considered a fixed  
 175 function of  $A_c$  ( $0.006 \cdot A_c$ ), because it performed better in our daily model than  
 176 exponential formulations as a function of temperature (Sala & Tenhunen 1996; De Pury  
 177 & Farquhar 1997; Bernacchi et al. 2001). Following De Pury & Farquhar (1997):

$$W_c(i) = \frac{V_{cmax}(i) \cdot (C_i(i) - \Gamma(i))}{C_i(i) + K_c(i) \left(1 + \frac{[O_2]}{K_o(i)}\right)} \quad [E1],$$

$$W_j(i) = \frac{J_{max}(i) \cdot (C_i(i) - \Gamma(i))}{4C_i(i) + 8\Gamma(i)} \quad [E2];$$

178 where  $C_i$  is the CO<sub>2</sub> intercellular concentration,  $\Gamma$  is the [CO<sub>2</sub>] compensation point for  
 179 photosynthesis in the absence of dark respiration, and  $K_c$  and  $K_o$  are the kinetic  
 180 Michaelis-Menten constants for carboxylation and oxygenation, respectively.  $V_{cmax}$  and  
 181  $J_{max}$  are temperature dependent parameters as follows. Photosynthesis is known to  
 182 respond to the carbon concentration within chloroplasts  $C_c$  rather than to  $C_i$ . We keep  
 183 through the paper the notation presented here in [E1] and [E2] but discuss below how  
 184 mesophyll conductance is taken into account empirically in relation to water stress  
 185 when calculating  $g_s$  and acknowledge the possible limitations of our approach  
 186 (Reichstein et al. 2002; Grassi & Magnani 2005; Flexas et al. 2006; Sun et al. 2014).

187 Climate influences leaf photosynthesis calculations through the temperature  
 188 dependence of different parameters (Bernacchi et al. 2001; Nobel 2009).  $\Gamma$ ,  $K_c$  and  $K_o$   
 189 were modelled using Arrhenius functions of daily mean temperature ( $T_{day}$ , in °C) with  
 190 parameters as in De Pury & Farquhar (1997). We modelled  $J_{max}$  as a fixed rate of  $V_{cmax}$   
 191 ( $J_{max}(i) = J_{coef} \cdot V_{cmax}(i)$ ) after comparing with different temperature dependent

192 formulations (De Pury & Farquhar 1997; Maseyk et al. 2008). The model behaviour  
 193 was better when the temperature dependence of  $V_{cmax}$  was modelled using a logistic  
 194 function (Gea-Izquierdo et al. 2010) rather than an exponential function as in Misson  
 195 (2004):

$$V_{cmax}(i) = \frac{V_{max}}{(1 + \exp(V_b \cdot ((T_{day}(i) + 273) - V_{ip})))} \cdot \theta_p \quad [E3];$$

196  $V_{max}$ ,  $V_b$  and  $V_{ip}$  are parameters to be estimated, with  $V_{max}$  being the asymptote and  $V_{ip}$   
 197 the inflection point.  $\theta_p$  is a soil water stress function dependent on soil moisture  
 198 conditions of the previous year. It takes into account down-regulation of photosynthesis  
 199 in response to protracted drought through its impact on the photosynthetic capacity of  
 200 active LAI in evergreen species caused by constraints in  $V_{cmax}$  produced by irreversible  
 201 photoinhibition, modifications in leaf stoichiometry and/or aging of standing foliage  
 202 through lower leaf replacement rates in response to long-term water stress (Sala &  
 203 Tenhunen 1996; Niinemets & Valladares 2004; Niinemets 2007; Vaz et al. 2010).  
 204  $\theta_p = 1 - \exp(p_{str} \cdot SWC_{180})$  [E4], where  $p_{str}$  is a parameter to be estimated and  
 205  $SWC_{180}$  is the mean soil water content (mm) from July to December of the previous  
 206 year.

207 Photosynthesis is coupled to stomatal conductance calculation, which is estimated  
 208 using a modified version of the Leuning (1995) equation:

$$g_s(i) = \frac{g_1 \cdot A_n(i)}{(C_s(i) - \Gamma(i)) \cdot (1 + VPD(i)/VPD_0)} \cdot \theta_g(i) \quad [E5],$$

209  $g_1$  and  $VPD_0$  are parameters,  $VPD(i)$  is daily vapour pressure deficit,  $C_s$  is the leaf  
 210 surface [ $CO_2$ ];  $\theta_g$  is a non-linear soil water stress function as:

$$\theta_g(i) = \frac{1}{1 + \exp(soil_b \cdot (SWC(i) - soil_{ip}))} \quad [E6],$$

211  $soil_b$  and  $soil_{ip}$  are parameters and  $SWC(i)$  is daily soil water content (mm).  $\theta_g$  accounts  
 212 for variability in gas exchange under drought conditions which cannot be taken into  
 213 account only through stomatal control, e.g. related to mesophyll conductance or  
 214 stomatal patchiness. Therefore, with this empirical expression we partly represent the  
 215 effect of  $CO_2$  fractionation during mesophyll conductance under water stress,  
 216 acknowledging that this will be likely more complex under environmental stress  
 217 (Reichstein et al. 2002; Grassi & Magnani 2005; Flexas et al. 2006; Sun et al. 2014).  
 218 The coupled photosynthesis-stomatal conductance system of equations was estimated  
 219 separately for sun and shade leaves. Canopy photosynthesis was integrated using LAI  
 220 divided into its sunlit and shaded fractions (De Pury & Farquhar 1997). Transmission  
 221 and absorption of irradiance was calculated following the Beer-Lambert law as a  
 222 function of LAI, with  $LAI_{sun}=(1-\exp(-LAI))\cdot K_b$  ( $K_b$  is the beam light extinction  
 223 coefficient, which was set to 0.8) and  $LAI_{shade}=LAI-LAI_{sun}$  (Misson 2004). In the mixed  
 224 stand (Fontblanche), photosynthesis was calculated separately for *Q. ilex* and *P.*  
 225 *halepensis*, and then integrated to get stand estimates of forest productivity.

226

### 227 *Modelling the effect of climatic forcing on carbon allocation*

228 The model allocates daily carbon assimilated either to the canopy, stem, roots or  
 229 storage of non-structural carbohydrates (NSC) to mimic intra-annual carbohydrate  
 230 dynamics (Misson 2004; Dickman et al. 2014). Although trees can store carbon within  
 231 different above-ground and below-ground compartments (Millard et al. 2007), carbon  
 232 storage is treated as a single pool within the model. Tree autotrophic respiration ( $R_a$ ) is  
 233 modelled as a function  $f(i)$  of daily photosynthesis and maximum daily temperature  
 234 ( $T_{max}$ ) (Sala & Tenhunen 1996; Nobel 2009) as:

$$235 \quad R_a(i)=\max\{0.3, f(i)\}, \text{ with } f(i) = 0.47 \cdot A_n(i) \cdot (1 - \exp(p_{respi} \cdot T_{max}(i))) \quad [E7];$$

236 where  $p_{respi}$  is a parameter. Net photosynthesis is calculated for day  $i$  as  $A_N(i) = A_n(i) -$   
237  $R_d(i)$ . The model simulates several phenological phases during the year (see Figure 1):  
238 [P1] winter period where all photosynthates assimilated daily  $A_N(i)$  are allocated to the  
239 storage reservoir (NSCs) but there is no accumulation of growing degree days (GDD).  
240 [P2] winter period where all  $A_N(i)$  are allocated to storage (i.e. the same as in [P1]) but  
241 in opposition to [P1] there is active accumulation of GDD which define the threshold  
242  $GDD_l$  to trigger the next phenophase [P3] (budburst, leaf-flush).  
243 [P3] budburst, where carbon available  $C_T(i) = A_N(i) + C_{bud}$  ( $C_{bud}$  is daily C storage utilized  
244 from buds, a parameter) is either allocated to the canopy, to roots or to the stem.  
245 [P4] once the canopy has been completed in [P3], the next phenophase [P4] starts; in  
246 this period daily photosynthates  $A_N(i)$  are allocated either to the stem or to storage;  
247 [P5] the last phenophase [P5] starts when the photoperiod (parameter) crosses a  
248 minimum threshold in fall. In this phase root mortality occurs. Otherwise [P5] is similar  
249 to [P1] and [P2], in the sense that all  $A_N(i)$  is used for storage until next year [P3] starts.

250 Allocation of carbon to different plant compartments is complex because it can be  
251 decoupled from photosynthetic production depending on different factors, some of them  
252 climatic, acting at different temporal scales (Friedlingstein et al. 1999; Sala et al. 2012;  
253 Chen et al. 2013; McMurtrie & Dewar 2013). In this new version of the model we set  
254 the different allocation relationships as nonlinear functions of temperature and soil  
255 water content,  $h(i) = f_1(T_{max}) \cdot f_2(SWC)$ , in [P3] and [P4] following the functional  
256 relationships described in Gea-Izquierdo et al. (2013). This means that now we take into  
257 account homeostatic acclimation processes at the canopy level related to LAI  
258 dependence on water availability (Hoff & Rambal 1993; Sala & Tenhunen 1996;  
259 Reichstein et al. 2003). LAI is negatively related to long-term drought because litterfall  
260 is negatively linked to water stress (Limousin et al. 2009; Misson et al. 2011) and bud

261 size depends on climate influencing the period of bud formation (Montserrat-Marti et al  
 262 2009). Therefore the actual carbon that can be allocated to the canopy in [P3] of year j  
 263 ( $AlloC_{canopy}(j)$ ) was set as a function of previous year moisture conditions ( $\theta_{LAI}(j)$ ), and  
 264 maximum carbon that can be allocated to the canopy ( $MaxC_{canopy}$ ).  $MaxC_{canopy}$  is  
 265 calculated from  $LAI_{max}$  and  $SLA$ , and  $AlloC_{canopy}(j) = \theta_{LAI}(j) \cdot MaxC_{canopy}$ , where:

$$266 \quad \theta_{LAI}(j) = \left(1 - 2 \cdot \frac{p_{LAI} - SWC_{250}}{p_{LAI}}\right), \text{ constrained to } \theta_{LAI}(j) \in [0.7, 1.0] \quad [E8]$$

267  $p_{LAI}$  is a parameter to be calibrated representing the threshold over which  $\theta_{LAI}(j) = 1$   
 268 and  $SWC_{250}$  is mean soil water content for May-December of previous year.

269 Leaf turnover is variable within years and partly related to water availability  
 270 (Limousin et al. 2009, 2012). We considered a mean leaf turnover rate of 3 years for  
 271 pines and 2 for oaks. To model within year variability in leaf phenology (i.e. leaf  
 272 growth and litterfall) we followed Maseyk et al. (2008) and Limousin et al. (2009)  
 273 (Figure 1). C allocation to the canopy (i.e. including primary growth) in [P3] is  
 274 calculated as:  $C_{canopy}(i) = C_T(i) \cdot (1 - 0.2 \cdot h_{3\_1}(i)) \cdot Ratio_{root/leaf}$ ,  $Ratio_{root/leaf}$  was fixed to 1.5  
 275 for both species (Misson et al. 2004; Ourcival, unpublished data), and:

$$276 \quad h_{3\_1}(i) = (1 - \exp(p_{3moist} \cdot SWC(i))) \cdot \left( \exp\left(-0.5 \cdot \left(\frac{T_{max}(i) - p_{3temp}}{p_{3sd}}\right)^2\right) \right) \quad [E9],$$

277  $p_{3moist}$ ,  $p_{3temp}$  and  $p_{3sd}$  are parameters representing the scale of the  $SWC$  and the optimum  
 278 and dispersion of the  $T_{max}$  functions respectively. The carbon allocated to the stem  
 279 ( $C_{stem}$ ) in [P3] is  $C_{stem}(i) = C_T(i) \cdot 0.2 \cdot h_{3\_1}(i) \cdot h_{3\_2}(i)$ , where:

$$280 \quad h_{3\_2}(i) = (1 - \exp(st_{3moist} \cdot SWC(i))) \cdot \left( \exp\left(-0.5 \cdot \left(\frac{T_{max}(i) - st_{3temp}}{st_{3sd\_temp}}\right)^2\right) \right) \quad [E10];$$

281 with  $h_{3\_1}(i)$  as in [E9];  $st_{3moist}$ ,  $st_{3temp}$  and  $st_{3sd\_temp}$  are parameters as in  $h_{3\_1}(i)$ . The  
 282 carbon allocated to roots in [P3] is set complementary to that of the other compartments  
 283 to close the carbon budget within the tree, i.e.:  $C_{roots}(i) = C_T(i) - C_{stem}(i) - C_{canopy}(i)$ .



283 Finally, in [P4] carbon assimilated daily  $A_N(i)$  is allocated either to stem growth or  
 284 to storage until changing to [P5]. There since in [P1] and [P2] again all  $A_N(i)$  is only  
 285 allocated to storage until [P3] next year (Misson 2004). In [P4], the amount of carbon to  
 286 be allocated to stem growth is now also set as a function of climatic forcing:

287  $C_{stem}(i) = A_N(i) \cdot (1 - h_4(i))$  and  $C_{stor}(i) = A_N(i) \cdot h_4(i)$ , with:

$$288 \quad h_4(i) = \left(1 - \exp(st_{4temp} \cdot T_{max}(i)) \cdot \left(\exp\left(-0.5 \cdot \left(\frac{SWC(i)}{st_{4sd\_moist}}\right)^2\right)\right)\right) \quad [E11];$$

289  $st_{4temp}$  and  $st_{4sd\_temp}$  are parameters as from [E10].

290

### 291 *Eddy covariance CO<sub>2</sub> flux and dendrochronological data*

292 The process-based model was calibrated using daily gross primary productivity  
 293 (GPP), dendrochronological data and inventory data. To develop the model, in a first  
 294 step those functions used to model daily stand photosynthesis (i.e. [E1] to [E9]) were  
 295 calibrated against GPP values. GPP estimates were obtained from half-hourly net CO<sub>2</sub>  
 296 flux measurements (NEP). GPP was obtained as the difference between measured net  
 297 ecosystem productivity and calculated ecosystem respiration (Reichstein et al. 2005).  
 298 Negative GPP values were corrected following Schaefer et al. (2012). Half-hourly GPP  
 299 data were integrated to obtain daily estimates for the period 2001-2013 (Puechabon,  
 300 methods detailed in Allard et al. (2008)) and 2008-2012 (Fontblanche) (Table 1).

301 In a second step, those functions used to model how carbon assimilated and/or  
 302 storage is allocated to growth of the tree stem (i.e. [E10] and [E11]) were developed  
 303 using calculated annual stem biomass increment time series. Stem biomass increment  
 304 chronologies were built combining dendroecological data and forest inventory data  
 305 collected at each site. We built one chronology for *Q. ilex* in Puechabon, a second for *Q.*  
 306 *ilex* in Fontblanche and a third one for *P. halepensis* at Fontblanche (Figure 2). For  
 307 pines, two perpendicular cores were extracted using an increment borer from 25 trees in

308 fall 2013 whereas for oaks we used crosssections. In Fontblanche, 15 oak stems were  
309 felled and basal sections collected in spring 2014. A total of 17 oak stems from  
310 Puechabon were logged in 2005 and 2008. The age and diameter distributions of the  
311 studied forests are depicted in Figure A2.

312 All samples were processed using standard dendrochronological methods (Fritts  
313 1976). Annual growth (RW) was measured using a stereomicroscope and a moving  
314 table switched to a computer. RW crossdating was visually and statistically verified.  
315 RW estimates were transformed to basal area increments (BAI,  $\text{cm}^2 \cdot \text{year}^{-1}$ ). Mean BAI  
316 chronologies were obtained by averaging individual tree BAI time series. In  
317 Fontblanche BAI during the period 1987-1995 was standardized relative to the mean  
318 calculated after excluding that period (Figure 2). BAI data were standardized because  
319 we did not find a climatic explanation for the abrupt growth peak observed in  
320 Fontblanche during that period (Figure 2). Therefore we assumed that it had been  
321 caused by a release event (i.e. reduction in competition) produced by the death of  
322 neighbours as a consequence of winter frost during 1985 and 1987 (Vennetier, pers.  
323 comm., 2014). These two frosts were reflected by the presence of characteristic frost  
324 rings in most individuals from Fontblanche.

325 To scale BAI chronologies to the same units as annual stem biomass (which is an  
326 output of the model) we used plot inventory data collected around the flux towers at the  
327 two sites. Inventory data included stem diameter for all trees and tree height collected  
328 for a subsample every two years during 2007-2011 in Fontblanche, and annual diameter  
329 estimates for the period 1986-2011 for Puechabon. Individual annual biomass  
330 increments were estimated by subtracting stem biomass at consecutive years and then  
331 stand stem biomass increment (SBI,  $\text{g C m}^{-2} \cdot \text{year}^{-1}$ ) built integrating plot data. Stem  
332 biomass was calculated using allometric functions. For pines, we calculated stem

333 biomass using diameter and estimated stem height assuming that the tree bole follows a  
334 paraboloid shape (Li et al. 2014). For oaks, stem biomass was calculated following  
335 Rambal et al. (2004). Once SBI had been estimated for the years when we had available  
336 inventory data, BAI chronologies were correlatively scaled to SBI units ( $\text{g C m}^{-2}\cdot\text{year}^{-1}$ ).  
337 We built two mean stand SBI chronologies, one for each site, meaning that we  
338 analysed carbon allocation within stands, not differentiating between species in  
339 Fontblanche. These two SBI chronologies were used to calibrate sitewise [E10] and  
340 [E11].

341

#### 342 *Model development and analyses*

343 Parameters were selected according to the ecological characteristics of the species,  
344 exploring the model using comprehensive sensitivity analysis to sequentially optimize  
345 groups of parameters. In a first step, a group of common parameters (those included in  
346 [E2] to [E8]) was selected using GPP data from Fontblanche (Table 2). The species-  
347 dependent parameters selected for *Q. ilex* in this first step were independently validated  
348 when applied in Puechabon (those in Table 2 common for the two sites). In a second  
349 step, a subset of site-dependent parameters was calibrated against GPP and SBI data.  
350 Four from [E6] and [E9] were calibrated using GPP data, and five parameters in [E10]  
351 and [E11] were calibrated using stem biomass increment data (Table 2). The local  
352 parameters were calibrated constrained to an ecologically realistic range using a global  
353 optimization algorithm and maximum likelihood principles (Gaucherel et al. 2008).

354 To compare model output with stem biomass chronologies as estimated from  
355 dendroecological data we used only the period where we had available daily  
356 meteorological data (1960-2013), which was also a period that did not include juvenile  
357 years with increasing BAI (BAIs reached an asymptote after increasing the first 15-20

358 juvenile years, Figure 2). The model does not take into account how size differences in  
359 allometry or ontogeny affect carbon allocation (Chen et al. 2013). We tried to keep the  
360 model as simple as possible also because we had no such data to calibrate ontogenic  
361 effects. Hence the model is designed for non-juvenile stands with canopies that reached  
362 a steady state with asymptotic  $LAI_{max}$ . For the same reasons it does not take into  
363 account how changes in management affect carbon allocation. The model was analysed  
364 in terms of goodness of fit. Additionally, for the period where we had available daily  
365 meteorological data we simulated time series of GPP, ecosystem water use efficiency  
366 ( $WUE = GPP/ET$ , with  $ET$ =actual evapotranspiration) and intrinsic water use  
367 efficiency of sun leaves ( $iWUE = A_N/g_s$ ) calculated following Beer et al. (2009).

368

369

## Results

370 The studied evergreen forests exhibit a bimodal pattern in GPP with maxima in  
371 spring and autumn (Figure 3) as often observed in Mediterranean ecosystems (e.g.  
372 Baldocchi et al. 2010). GPP was above zero almost every day of the year, including  
373 winter, particularly in the milder site, Fontblanche (Table 1). This means that there is  
374 active photosynthesis all year round in these evergreen forests, including both periods of  
375 climatic stress with low temperature and short photoperiod in winter, and with low  
376 moisture availability in summer (Figure 3). Mean annual GPP was  $1431.4 \pm 305.4 \text{ g C m}^{-2}$   
377  $\text{year}^{-1}$  and precipitation  $642.7 \pm 169.7 \text{ mm}$  in Fontblanche; whereas it was  $1207.3 \pm 206.7$   
378  $\text{g C m}^{-2} \text{ year}^{-1}$  and  $1002.6 \pm 328.2 \text{ mm}$  in Puechabon (see Table 1 for more details). Mean  
379 GPP was higher at Fontblanche because carbon assimilation was greater in the low  
380 temperature winter period but similar the rest of the year (Figure 3). Stem growth did  
381 not show any long-term (decadal) growth trend for any of the species studied (Figure 2).

382 The model accurately represented the low frequency response of GPP: both the  
383 seasonal variability in GPP within years and variability in GPP among years (Figure 4).  
384 The model explained over 50% of the annual biomass growth variance, and 46% and  
385 59% of daily GPP in Fontblanche and Puechabon, respectively (Figure 4). This means  
386 that we were able to mimic the daily, seasonal and long-term trends in stand  
387 productivity with unbiased estimates but also to model how carbon is allocated to stem  
388 growth along the year at the different phenophases described. The model assumed  
389 species-specific carbon allocation responses set to the different plant compartments as  
390 nonlinear functions of temperature and soil moisture. These relationships were  
391 biologically meaningful in the sense that photosynthesis and carbon allocation could be  
392 decoupled to some extent as a function of climatic variability. Once the canopy has been  
393 formed in spring, the model allocated more carbon to the stem and less to storage when  
394 less severe stress occurs, i.e. with decreasing temperatures and more humid conditions  
395 (Figure 5).

396 Both sites exhibited an increase in temperature particularly evident in the maximum  
397 values but only Puechabon suffered a decrease in annual precipitation between 1960 and  
398 2012 (Figure A1). In the model, the studied forests acclimated to changing climatic  
399 conditions in the last decades coupling different physiological traits and simulated  
400 annual GPP greatly followed the overall trends in precipitation observed. In  
401 Fontblanche, which is milder and receives less precipitation, GPP remained stable since  
402 the 1960s and presented no apparent long-term trend (Figure 6). In contrast, in the  
403 coldest and rainiest site (Puechabon) the model simulated a decrease in GPP (Figure 6),  
404 which was driven by the prevailing decrease in precipitation observed since the 1960s  
405 (Figure A1). This reduction of GPP was partly a consequence of decreased LAI in  
406 response to enhanced long-term water stress (Figure A3; Limousin et al. 2009; Misson

407 et al. 2011). Simulated long-term decadal trends in mean annual stomatal conductance  
408 were similar and decreasing at the two sites with greater water stress as a consequence  
409 of enhanced temperatures (Figure 6). The two species studied showed a long-term  
410 increase in simulated iWUE (Figure 7) following the decrease in simulated  $g_s$  (Figure  
411 6). The interannual variability of WUE and iWUE were highly and positively correlated  
412 (Figure 7). However, in the long-term they followed a different pattern particularly in  
413 Puechabon where there was a recent decline in WUE (not observed in iWUE) forced by  
414 trends in ET and GPP (Figure 7). This means that the recent reduction in simulated GPP  
415 was proportionally greater than that of simulated ET (Figure 6; Figure A3).

416

417

## Discussion

418 *Linking photosynthetic production to carbon allocation as a function of climate*

419 The model calculates stand productivity and carbon allocation to stem growth in  
420 response to climate and  $[CO_2]$  with realism. It is particularly well suited to mimic the  
421 effect of water stress in plant performance by the explicit assessment of different  
422 acclimation processes at the canopy level including changes in stomatal conductance  
423 and photosynthetic capacity (Sala & Tenhunen 1996; Reichstein et al. 2003; Limousin  
424 et al. 2010; Misson et al. 2011). Additionally, the model simulates carbohydrate storage  
425 dynamically as a function of environmental variability. Climate can affect differently  
426 the carbon dynamics and pattern of C-allocation to different tree compartments at  
427 different phenophases. In the model the storage reservoir is an active sink for  
428 assimilated carbon during some periods of the year and a source in spring to be used in  
429 primary and secondary growth (Figure A5). Additionally stem growth is limited by  
430 climatic constraints (in [P3] and [P4]) rather than just by the amount of available  
431 carbohydrates (Millard et al. 2007). This means that water stress and optimum

432 temperature directly affect the modelled processes assuming that cell-wall expansion in  
433 the xylem can relate to climatic variability differently than photosynthetic production  
434 (Sala et al. 2012). The model showed C-limitation (for primary growth) the years when  
435  $LAI_{max}$  was not achieved (i.e. a limitation in LAI is driven by limitations in the C supply  
436 in spring), e.g. all years in Puechabon for the period shown in Figure A5 (1995-2012)  
437 but only those years in Fontblanche when the minimum value considered as a threshold  
438 was reached. Therefore both C-source (photosynthesis) and C-sink (just related to  
439 growth, other sinks such as volatile organic compounds or root exudates are not  
440 explicitly included in the model) limitations can be assessed at different years within  
441 one site and even at different periods within the same year (Millard et al. 2007; Sala et  
442 al. 2012; Chen et al. 2013; Fatichi et al. 2014). This hypothesis seems plausible as  
443 drought stress affects both C-source (e.g. through reduced stomatal conductance) and C-  
444 sink limitations (e.g. cell water turgor, hydraulic performance) (McDowell et al. 2013).  
445 Whether the pattern of C-storage simulated is realistic is something that needs to be  
446 validated against actual data. However, the flexible way in which stored C is modelled  
447 has much potentiality to improve ecosystem models that only view a carbon-source  
448 limitation (Sala et al. 2012; Friend et al. 2014).

449 Water stress is generally considered the greatest limitation for Mediterranean  
450 ecosystems, driving an intimate relation between precipitation and both growth and  
451 photosynthesis (Breda et al. 2006; Pereira et al. 2007; Baldocchi et al. 2010; Gea-  
452 Izquierdo & Cañellas 2014). Our results show that a long-term decrease in precipitation  
453 triggered a decrease in simulated GPP at the more rainy and continental site. However,  
454 this decline was not expressed in the growth-trends. This means that long-term  
455 productivity and allocation of C to secondary growth were decoupled and did not match  
456 (Sala et al. 2012; Chen et al. 2013; Fatichi et al. 2014). The existence of trade-offs

457 between carbon assimilation and allocation in relation to environmental variability  
458 suggests caution when using growth as a direct proxy to investigate stand productivity  
459 dynamics (e.g. Piovesan et al. 2008; Peñuelas et al. 2008; Gea-Izquierdo & Cañellas  
460 2014). GPP was greater in the site receiving less precipitation, which could be related to  
461 differences in soil retention capacity. However both soils are calcareous, shallow and  
462 stony and differences in GPP were greatly explained by less limitation for carbon  
463 assimilation of low winter temperatures at the warmest site (Fontblanche). They can  
464 also be a result of different species composition (oak vs. pine-oak). LAI is greater at the  
465 site yielding higher annual GPP. Nonetheless, had this factor been responsible for the  
466 observed differences in winter photosynthesis, there would have also been differences  
467 in spring photosynthesis, which was not the case (Figure 3).

468 A better understanding of the underlying processes determining carbon allocation  
469 will benefit process-based models (Sala et al. 2012; Fatichi et al. 2014). Model  
470 parameters were within the range found in the literature, bearing in mind that using a  
471 daily time step to study differential processes or not distinguishing between leaf ages  
472 will affect the scaling of parameters such as  $J_{max}/V_{cmax}$  or  $R_d$  (De Pury & Farquhar 1997;  
473 Grassi & Magnani 2005; Masseyk et al. 2008; Vaz et al. 2010). Daily climatic data are  
474 readily available at a greater spatial scale than data with a higher temporal resolution,  
475 which increases applicability of daily models. Model performance could be improved  
476 by addressing respiration changes related to ontogeny and allometry, nutrient limitations  
477 (e.g. N/P) on photosynthesis, or including more complex up-scaling of leaf-level  
478 photosynthesis (Niinemets et al. 1999; Niinemets 2007; Chen et al. 2013; McMurtrie &  
479 Dewar 2013). However, it is difficult to find suitable data to calibrate such processes.  
480 Similarly, it would be challenging to include allocation to reproductive effort in the  
481 carbon budget. This is because, even if it is influenced by water stress in the studied



482 forests (Pérez-Ramos et al. 2010), there is still great uncertainty in the causal factors  
483 driving multi-annual variability in fruit production (Koenig and Knops 2000).  
484 Addressing stand dynamics would also help to generalize model applicability. Stand  
485 disturbances modifying stand competition can leave an imprint in growth for more than  
486 a decade whereas they do not seem to affect stand GPP over more than one or two years  
487 if the disturbance is moderate (Misson et al. 2005; Granier et al. 2008). In response to  
488 changes in competition the trees modify carbon allocation or keep the root:shoot ratio  
489 constant to enhance productivity on a per-tree basis but up to an asymptotic stand GPP.  
490 Still, the model behaviour was good compared with other studies that addressed  
491 ontogenic changes in the carbon-allocation response to photosynthesis (Li et al. 2014)  
492 and similar or better than that of other mechanistic approaches calibrated to  
493 standardized dendroecological data (Misson et al. 2004; Evans et al. 2006; Gaucherel et  
494 al. 2008; Tolwinski-Ward et al. 2011; Touchan et al. 2012).

495

#### 496 *Forest performance in response to recent climate change and [CO<sub>2</sub>] enhancement*

497 Few studies under natural conditions observed a net increase of growth rates in  
498 response to enhanced CO<sub>2</sub> levels since the late 1800s, meaning that other factors such as  
499 water stress and/or N/P were more limiting for photosynthesis and/or allocation to  
500 growth than [CO<sub>2</sub>] (Niinemets et al. 1999; Peñuelas et al. 2011; McMurtrie & Dewar  
501 2013; Lévesque et al. 2014). Yet the forests have increased their iWUE. This can be  
502 partly a passive consequence of enhanced [CO<sub>2</sub>] but higher iWUE observed in more  
503 water stressed sites suggests that climate is co-responsible for an active acclimation of  
504 physiological plant processes (Keenan et al. 2013; Leonardi et al. 2013; Saurer et al.  
505 2014). These processes would include a higher stomatal control like in our results where  
506 in turn we did not observe any increase in long-term carbon assimilation. The mean

507 annual stomatal conductance simulated was driven by climate but also decreased  
508 simultaneously in time with increasing  $[\text{CO}_2]$  (Appendix A4). Furthermore, there is  
509 debate on whether there has been an increase in ecosystem WUE in response to recent  
510 changes in  $[\text{CO}_2]$  under a warming climate (Beer et al. 2009; Reichstein et al. 2002;  
511 Keenan et al. 2013). In our results the high-frequency of WUE followed that of  $i\text{WUE}$ ,  
512 but there was some mismatch between the two traits in the low-frequency. We observed  
513 an increase in simulated annual WUE for the period 1980-2000 at the site where  
514 precipitation remained stable, whereas there was a decrease in WUE following that in  
515 GPP particularly evident in the site experiencing a drier climate in recent years. This  
516 trend was not observed in  $i\text{WUE}$ , which means that reductions in GPP and  $g_s$  were  
517 proportionally greater than those in ET (Figure 6, Figure 7, Appendix A3).

518 Higher  $\text{CO}_2$  concentrations enhance photosynthesis with the equations used to  
519 calculate leaf photosynthesis in biochemical models (e.g. Gaucherel et al. 2008; Keenan  
520 et al. 2011; Leonardi et al. 2013; Boucher et al. 2014). Thus, the absence of a long-term  
521 increase in GPP and growth would not mean that enhanced  $[\text{CO}_2]$  was not beneficial for  
522 model outputs (particularly in the case of C-source limitation) but that the net control  
523 exerted by other factors such as climatically driven stress was more limiting than that of  
524  $[\text{CO}_2]$  availability: growth and photosynthesis would have been lower had we used  
525 constant  $[\text{CO}_2]$  with the same model parameters. The absence of any modification in the  
526 growth trends, even if there is changes in WUE, would express sink limitation mostly  
527 related to hydraulic constraints (Peñuelas et al. 2011; Sala et al. 2012; Keenan et al.  
528 2013). Often, the trees express a growth decline at those sites where there is an  
529 enhancement in long-term water stress that dominates species performance (e.g. Bigler  
530 et al. 2006; Piovesan et al. 2008; Gea-Izquierdo et al. 2014). In contrast, it has been  
531 observed under certain conditions that trees have increased growth with warming since

532 the 1850s (Salzer et al. 2009; Gea-Izquierdo & Cañellas 2014). These studies suggest  
533 the existence of a positive effect of warming rather than that of [CO<sub>2</sub>] fertilization upon  
534 growth in forests where water stress is not the most limiting factor. Our study sites are  
535 located within the Northern limit of the Mediterranean Region, meaning that the two  
536 species studied occupy drier and warmer areas more to the South. The two species have  
537 different functional characteristics, e.g. oaks are anisohydric whereas pines tend to be  
538 isohydric. This confers them different capacities of adaptation to climate change, which  
539 means that they should play different roles in future stand dynamics. Our results express  
540 the existence of trade-offs in response to climate at different phenological periods. This  
541 is important since synergistic environmental stresses acting at different periods can  
542 trigger tree mortality (McDowell et al. 2013; Voltas et al. 2013). Model sensitivity  
543 analysis could be performed to discuss the influence of specific factors such as climate  
544 or [CO<sub>2</sub>] causing instability in the climate-growth response (D'Arrigo et al. 2008;  
545 Boucher et al. 2014). However [CO<sub>2</sub>] enhancement and climate warming are mixed in  
546 analysis performed using data from field studies, which can make the isolation of their  
547 effect problematic. The model can be applied using abundant dendrochronological data  
548 used to determine the site-dependent parameters. This would give much flexibility to  
549 investigate growth trends and forest performance in response to global change at a  
550 larger scale.

551

## 552 **Conclusions**

553 By developing an original process-based model with carbon allocation relationships  
554 explicitly expressed as functions of climate we accurately simulated gross primary  
555 productivity and allocation of carbon to secondary growth in evergreen Mediterranean  
556 forests. Different processes were modelled as functions of environmental variability,

557 including CO<sub>2</sub> and climate. The studied forests expressed trade-offs in carbon allocation  
558 to different plant compartments in response to stress in different seasons, namely with  
559 low temperatures and a short photoperiod in winter, and with moisture shortage in  
560 summer. We modelled a decreasing time trend in stomatal conductance, which would  
561 suggest a partly active increase of iWUE in the forests studied. Interannual variability in  
562 WUE followed closely that of iWUE. However, WUE exhibited a decreasing trend at  
563 the site where we simulated a decrease in LAI and GPP in response to a decrease in  
564 annual precipitation since the 1980s. Long-term GPP remained at similar levels in the  
565 last 50 years just in one stand whereas it declined in the forest suffering a reduction in  
566 precipitation. This suggests different acclimation processes at the canopy level and in  
567 the pattern of allocation in response to enhanced xericity and increasing CO<sub>2</sub> levels,  
568 which could not counterbalance the negative effect of warming just in one site. Tree  
569 growth was partly decoupled from stand productivity, highlighting that it can be risky to  
570 accept growth as a direct proxy to GPP. The model is flexible enough to assess both C-  
571 source and C-sink limitations and includes a dynamic estimation of stored C. These  
572 features would improve ecosystem models with a fixed C-source formulation. By  
573 calibrating a limited number of parameters related to carbon allocation the model has  
574 great potential to be used with abundant dendroecological data to characterise past  
575 instability in the growth response in relation to environmental variability and simulate  
576 future forest response under different climatic scenarios.

577

## 578 **Acknowledgements**

579 G.G.I was funded by the Labex OT-Med (n° ANR-11-LABEX-0061) from the  
580 «Investissements d’Avenir» program of the French National Research Agency through  
581 the A\*MIDEX project (n° ANR-11-IDEX-0001-02). Federation de Recherche FR3098

582 ECCOREV, the labex IRDHEI and OHM-BMP also supported the study. We are  
583 grateful to Roland Huc for sharing data from Fontblanche.

584

585 **References**

586 Allard, V., Ourcival, J. M., Rambal, S., Joffre, R. and Rocheteau, A.: Seasonal and  
587 annual variation of carbon exchange in an evergreen Mediterranean forest in  
588 southern France, *Glob. Chang. Biol.*, 14(4), 714–725, 2008.

589 Baldocchi DD: Assessing the eddy covariance technique for evaluating carbon dioxide  
590 exchange rates of ecosystems: Past, present and future. *Glob. Chang. Biol.*, 9, 479–  
591 492, 2003.

592 Baldocchi, D. D., Ma, S. Y., Rambal, S., Misson, L., Ourcival, J. M., Limousin, J. M.,  
593 Pereira, J. and Papale, D.: On the differential advantages of evergreenness and  
594 deciduousness in mediterranean oak woodlands: a flux perspective, *Ecol. Appl.*,  
595 20(6), 1583–1597, 2010.

596 Beer, C., Ciais, P., Reichstein, M., Baldocchi, D., Law, B. E., Papale, D., Soussana, J.-  
597 F., Ammann, C., Buchmann, N., Frank, D., Gianelle, D., Janssens, I. a., Knohl, a.,  
598 Köstner, B., Moors, E., Rouspard, O., Verbeeck, H., Vesala, T., Williams, C. a. and  
599 Wohlfahrt, G.: Temporal and among-site variability of inherent water use efficiency  
600 at the ecosystem level, *Global Biogeochem. Cycles*, 23(2), 2009.

601 Bernacchi, C. J., Singsaas, E. L., Pimentel, C., Portis, A. R. and Long, S. P.: Improved  
602 temperature response functions for models of Rubisco-limited photosynthesis, *Plant*  
603 *Cell Environ.*, 24(2), 253–259, 2001.

604 Bigler, C., Braker, O. U., Bugmann, H., Dobbertin, M. and Rigling, A.: Drought as an  
605 inciting mortality factor in Scots pine stands of the Valais, Switzerland,  
606 *Ecosystems*, 9(3), 330–343, 2006.

607 Boucher, É., Guiot, J., Hatté, C., Daux, V., Danis, P. -a. and Dussouillez, P.: An inverse  
608 modeling approach for tree-ring-based climate reconstructions under changing  
609 atmospheric CO<sub>2</sub> concentrations, *Biogeosciences*, 11(12), 3245–3258, 2014.

610 Breda, N., Huc, R., Granier, A. and Dreyer, E.: Temperate forest trees and stands under  
611 severe drought: a review of ecophysiological responses, adaptation processes and  
612 long-term consequences, *Ann. For. Sci.*, 63(6), 625–644, 2006.

613 Breshears, D. D., Myers, O. B., Meyer, C. W., Barnes, F. J., Zou, C. B., Allen, C. D.,  
614 McDowell, N. G. and Pockman, W. T.: Tree die-off in response to global change-  
615 type drought: mortality insights from a decade of plant water potential  
616 measurements, *Front. Ecol. Environ.*, 7(4), 185–189, 2009.

617 Chen, G., Yang, Y. and Robinson, D.: Allocation of gross primary production in forest  
618 ecosystems: allometric constraints and environmental responses. *New Phytol.*,  
619 200(1176-1186), 2013.

620 D'Arrigo, R., Wilson, R., Liepert, B. and Cherubini, P.: On the “Divergence Problem”  
621 in Northern Forests: A review of the tree-ring evidence and possible causes, *Glob.*  
622 *Planet. Change*, 60(3-4), 289–305, 2008.

623 De Pury, D.G.G. and Farquhar, G.D.: Simple scaling of photosynthesis from leaves to  
624 canopies without the errors of big-leaf models. *Plant Cell Environ.*, 20(5), 537–557,  
625 1997.

626 De Kauwe, M. G., Medlyn, B. E., Zaehle, S., Walker, A. P., Dietze, M. C., Hickler, T.,  
627 Jain, A. K., Luo, Y. Q., Parton, W. J., Prentice, I. C., Smith, B., Thornton, P. E.,  
628 Wang, S. S., Wang, Y. P., Warlind, D., Weng, E. S., Crous, K. Y., Ellsworth, D. S.,  
629 Hanson, P. J., Seok Kim, H., Warren, J. M., Oren, R. and Norby, R. J.: Forest water  
630 use and water use efficiency at elevated CO<sub>2</sub>: a model-data intercomparison at two

631 contrasting temperate forest FACE sites, *Glob. Chang. Biol.*, 19(6), 1759–1779,  
632 2013.

633 Dickman, L. T., McDowell, N. G., Sevanto, S., Pangle, R. E. and Pockman, W. T.:  
634 Carbohydrate dynamics and mortality in a piñon-juniper woodland under three  
635 future precipitation scenarios., *Plant. Cell Environ.*, 2014.

636 Evans, M. N., Reichert, B. K., Kaplan, A., Anchukaitis, K. J., Vaganov, E. A., Hughes,  
637 M. K. and Cane, M. A.: A forward modeling approach to paleoclimatic  
638 interpretation of tree-ring data, *J. Geophys. Res.*, 111(G3), 2006.

639 Farquhar, G.D., von Caemmerer, S. and Berry, J.A.: A biochemical model of  
640 photosynthetic CO<sub>2</sub> assimilation in leaves of C3 species, *Planta*, 149(1), 78–90,  
641 1980.

642 Fatichi, S., Leuzinger, S. and Körner, C.: Moving beyond photosynthesis : from carbon  
643 source to sink-driven vegetation modeling, *New Phytol.*, 201, 1086–1095, 2013.

644 Flexas, J., Bota, J., Galmes, J., Medrano, H. and Ribas-Carbo, M.: Keeping a positive  
645 carbon balance under adverse conditions: responses of photosynthesis and  
646 respiration to water stress, *Physiol. Plant.*, 127(3), 343–352, 2006.

647 Friedlingstein, P., Joel, G., Field, C. B. and Fung, I. Y.: Toward an allocation scheme  
648 for global terrestrial carbon models, *Glob. Chang. Biol.*, 5(7), 755–770, 1999.

649 Fritts, H.C.: *Tree Rings and Climate*. Blackburn Press, 567 p, 1976

650 Gauchere, C., Campillo, F., Misson, L., Guiot, J. and Boreux, J. J.: Parameterization of  
651 a process-based tree-growth model: Comparison of optimization, MCMC and  
652 Particle Filtering algorithms, *Environ. Model. Softw.*, 23(10-11), 1280–1288, 2008.

653 Gea-Izquierdo, G., Mäkelä, A., Margolis, H., Bergeron, Y., Black, T. A., Dunn, A.,  
654 Hadley, J., Kyaw Tha Paw U, Falk, M., Wharton, S., Monson, R., Hollinger, D. Y.,  
655 Laurila, T., Aurela, M., McCaughey, H., Bourque, C., Vesala, T. and Berninger, F.:

656 Modeling acclimation of photosynthesis to temperature in evergreen conifer forests.  
657 *New Phytol.*, 188(1), 175–186, 2010.

658 Gea-izquierdo, G., Fernández-de-uña, L., Cañellas, I. Growth projections reveal local  
659 vulnerability of Mediterranean oaks with rising temperatures. *For. Ecol. Manage.*,  
660 305, 282–293, 2013.

661 Gea-Izquierdo, G. and Cañellas, I.: Long-term climate forces instability in long-term  
662 productivity of a Mediterranean oak along climatic gradients. *Ecosystems*, 17, 228–  
663 241, 2014.

664 Gea-Izquierdo, G., Viguera, B., Cabrera, M., Cañellas, I. Drought induced decline could  
665 portend widespread oak mortality at the xeric ecotone in managed Mediterranean  
666 pine-oak woodlands. *Forest Ecol. Manag.* 320, 70-82, 2014.

667 Granier, A., Breda, N., Longdoz, B., Gross, P. and Ngao, J.: Ten years of fluxes and  
668 stand growth in a young beech forest at Hesse, North-eastern France, *Ann. For. Sci.*,  
669 64 (7), 704, 2008.

670 Grassi, G. and Magnani, F.: Stomatal, mesophyll conductance and biochemical  
671 limitations to photosynthesis as affected by drought and leaf ontogeny in ash and  
672 oak trees, *Plant, Cell Environ.*, 28(7), 834–849, 2005.

673 Guiot, J., Boucher, E. and Gea-Izquierdo, G.: Process models and model-data fusion in  
674 dendroecology, *Front. Ecol. Evol.*, 2(August), 1–12, 2014.

675 Hoff, C. and Rambal, S.: An examination of the interaction between climate, soil and  
676 leaf area index in a *Quercus ilex* ecosystem, *Ann. For. Sci.*, 60(2), 153–161, 2003.

677 IPCC. *Climate Change: The Physical Science Basis. Summary for policymakers.*  
678 Stocker, T.F. et al. (Eds.) IPCC, Geneva, Switzerland. pp 33. 2013.



679 Keenan, T., Maria Serra, J., Lloret, F., Ninyerola, M. and Sabate, S.: Predicting the  
680 future of forests in the Mediterranean under climate change, with niche- and  
681 process-based models: CO<sub>2</sub> matters!, *Glob. Chang. Biol.*, 17(1), 565–579, 2011.

682 Keenan, T. F., Hollinger, D. Y., Bohrer, G., Dragoni, D., Munger, J. W., Schmid, H. P.  
683 and Richardson, A. D.: Increase in forest water-use efficiency as atmospheric  
684 carbon dioxide concentrations rise., *Nature*, 499(7458), 324–7, 2013.

685 Koenig, W. D. and Knops, M. H.: Patterns of annual seed production by Northern  
686 Hemisphere trees: a global perspective., *Am. Nat.*, 155(1), 59–69, 2000.

687 Körner, C., Basel, M.L. Growth Controls Photosynthesis – Mostly. *Nova Acta*  
688 *Leopoldina*, 283, 273–283, 2013.

689 Leonardi, S., Gentilesca, T., Guerrieri, R., Ripullone, F., Magnani, F., Mencuccini, M.,  
690 Noije, T. V and Borghetti, M.: Assessing the effects of nitrogen deposition and  
691 climate on carbon isotope discrimination and intrinsic water-use efficiency of  
692 angiosperm and conifer trees under rising CO<sub>2</sub> conditions, *Glob. Chang. Biol.*,  
693 18(9), 2925–2944, 2012.

694 Le Roux, X., Lacoite, A., Escobar-Gutierrez, A. and Le Dizes, S.: Carbon-based  
695 models of individual tree growth: A critical appraisal, *Ann. For. Sci.*, 58(5), 469–  
696 506, 2001.

697 Leuning, R.: A critical appraisal of a combined stomatal-photosynthesis model for C3  
698 plants. *Plant Cell Environ.* 18, 339-355, 1995

699 Lévesque, M., Siegwolf, R., Saurer, M., Eilmann, B. and Rigling, A.: Increased water-  
700 use efficiency does not lead to enhanced tree growth under xeric and mesic  
701 conditions., *New Phytol.*, 203(1), 94–109, 2014.

702 Li, G., Harrison, S. P., Prentice, I. C. and Falster, D.: Simulation of tree ring-widths  
703 with a model for primary production, carbon allocation and growth, *Biogeosciences*  
704 *Discuss.*, 11(7), 10451–10485, 2014.

705 Limousin, J. M., Rambal, S., Ourcival, J. M., Rocheteau, A., Joffre, R. and Rodriguez-  
706 Cortina, R.: Long-term transpiration change with rainfall decline in a Mediterranean  
707 *Quercus ilex* forest, *Glob. Chang. Biol.*, 15(9), 2163–2175, 2009.

708 Limousin, J. M., Longepierre, D., Huc, R. and Rambal, S.: Change in hydraulic traits of  
709 Mediterranean *Quercus ilex* subjected to long-term throughfall exclusion, *Tree*  
710 *Physiol.*, 30(8), 1026–1036, 2010.

711 Limousin, J.-M., Rambal, S., Ourcival, J.-M., Rodriguez-Calcerrada, J., Perez-Ramos, I.  
712 M., Rodriguez-Cortina, R., Misson, L. and Joffre, R.: Morphological and  
713 phenological shoot plasticity in a Mediterranean evergreen oak facing long-term  
714 increased drought, *Oecologia*, 169(2), 565–577, 2012.

715 Maseyk, K. S., Lin, T., Rotenberg, E., Grünzweig, J. M., Schwartz, A. and Yakir, D.:  
716 Physiology-phenology interactions in a productive semi-arid pine forest., *New*  
717 *Phytol.*, 178(3), 603–16, 2008.

718 McDowell, N.G., Fisher, R.A., Xu, C., Domec, J., Höltta, T., Mackay, D.S., Sperry, J.  
719 S., Boutz, A., Dickman, L., Gehres, N., Limousin, J.M., Macalady, A., Pangle, R.  
720 E., Rasse, D.P., Ryan, M.G., Sevanto, S., Waring, R.H., Williams, A.P., Yopez, E.  
721 A. and Pockman, W.T.: Evaluating theories of drought-induced vegetation mortality  
722 using a multimodel – experiment framework, *New Phytol.*, 200, 304–321, 2013.

723 McMurtrie, R. E. and Dewar, R. C.: New insights into carbon allocation by trees from  
724 the hypothesis that annual wood production is maximized, *New Phytol.*, 199(4),  
725 981–990, 2013.

726 Millard, P., Sommerkorn, M., Grelet, G.A. Environmental change and carbon limitation  
727 in trees: A biochemical, ecophysiological and ecosystem appraisal. *New*  
728 *Phytologist*, 175, 11–28, 2007.

729 Misson, L.: MAIDEN: a model for analyzing ecosystem processes in dendroecology.  
730 *Can. J. For. Res.*, 34, 874–887, 2004.

731 Misson, L., Rathgeber, C. and Guiot, J.: Dendroecological analysis of climatic effects  
732 on *Quercus petraea* and *Pinus halepensis* radial growth using the process-based  
733 MAIDEN model, *Can. J. For. Res.*, 34(4), 888–898, 2004.

734 Misson, L., Tang, J., Xu, M., Mckay, M. and Goldstein, A.: Influences of recovery from  
735 clear-cut , climate variability , and thinning on the carbon balance of a young  
736 ponderosa pine plantation, *Agric. Fore*, 130, 207–222, 2005.

737 Misson, L., Degueldre, D., Collin, C., Rodriguez, R., Rocheteau, A., Ourcival, J.-M.  
738 and Rambal, S.: Phenological responses to extreme droughts in a Mediterranean  
739 forest, *Glob. Chang. Biol.*, 17(2), 1036–1048, 2011.

740 Montserrat-Marti, G., Camarero, J. J., Palacio, S., Perez-Rontome, C., Milla, R.,  
741 Albuixech, J. and Maestro, M.: Summer-drought constrains the phenology and  
742 growth of two coexisting Mediterranean oaks with contrasting leaf habit:  
743 implications for their persistence and reproduction, *Trees-Structure Funct.*, 23(4),  
744 787–799, 2009.

745 Niinemets, U.: Photosynthesis and resource distribution through plant canopies., *Plant*  
746 *Cell Environ.*, 30(9), 1052–71, 2007.

747 Niinemets, U. and Valladares, F.: Photosynthetic acclimation to simultaneous and  
748 interacting environmental stresses along natural light gradients: optimality and  
749 constraints., *Plant Biol. (Stuttg.)*, 6(3), 254–68, 2004.

750 Niinemets, Ü., Tenhunen, J. D., Canta, N. R., Chaves, M. M., Faria, T., Pereira, J. S.  
751 and Reynolds, J. F.: Interactive effects of nitrogen and phosphorus on the  
752 acclimation potential of foliage photosynthetic properties of cork oak, *Q. suber*, to  
753 elevated atmospheric CO<sub>2</sub> concentrations, *Glob. Chang. Biol.*, 5, 455–470, 1999.

754 Nobel, P.S.: Physicochemical and environmental plant physiology. 4th edn. Academic  
755 Press, Elsevier, Oxford UK, 2009.

756 Peng, C. H., Guiot, J., Wu, H. B., Jiang, H. and Luo, Y. Q.: Integrating models with  
757 data in ecology and palaeoecology: advances towards a model-data fusion  
758 approach, *Ecol. Lett.*, 14(5), 522–536, 2011.

759 Peñuelas, J., Hunt, J. M., Ogaya, R. and Jump, A. S.: Twentieth century changes of tree-  
760 ring delta C-13 at the southern range-edge of *Fagus sylvatica*: increasing water-use  
761 efficiency does not avoid the growth decline induced by warming at low altitudes,  
762 *Glob. Chang. Biol.*, 14(5), 1076–1088, 2008.

763 Peñuelas, J., Canadell, J. G. and Ogaya, R.: Increased water-use efficiency during the  
764 20th century did not translate into enhanced tree growth, *Glob. Ecol. Biogeogr.*,  
765 20(4), 597–608, 2011.

766 Pereira, J. S., Mateus, J. A., Aires, L. M., Pita, G., Pio, C., David, J. S., Andrade, V.,  
767 Banza, J., David, T. S., Paco, T. A. and Rodrigues, A.: Net ecosystem carbon  
768 exchange in three contrasting Mediterranean ecosystems - the effect of drought,  
769 *Biogeosciences*, 4(5), 791–802, 2007.

770 Pérez-Ramos, I. M., Ourcival, J. M., Limousin, J. M. and Rambal, S.: Mast seeding  
771 under increasing drought: results from a long-term data set and from a rainfall  
772 exclusion experiment, *Ecology*, 91(10), 3057–3068, 2010.

773 Piovesan, G., Biondi, F., Di Filippo, A., Alessandrini, A. and Maugeri, M.: Drought-  
774 driven growth reduction in old beech (*Fagus sylvatica* L.) forests of the central  
775 Apennines, Italy, *Glob. Chang. Biol.*, 14(6), 1265–1281, 2008.

776 Rambal, S., Joffre, R., Ourcival, J. M., Cavender-Bares, J. and Rocheteau, a.: The  
777 growth respiration component in eddy CO<sub>2</sub> flux from a *Quercus ilex* mediterranean  
778 forest, *Glob. Chang. Biol.*, 10(9), 1460–1469, 2004.

779 Reichstein, M., Tenhunen, J. D., Rouspard, O., Ourcival, J. M., Rambal, S., Miglietta,  
780 F., Peressotti, A., Pecchiari, M., Tirone, G. and Valentini, R.: Severe drought effects  
781 on ecosystem CO<sub>2</sub> and H<sub>2</sub>O fluxes at three Mediterranean evergreen sites: revision  
782 of current hypotheses?, *Glob. Chang. Biol.*, 6(10), 999–1017, 2002.

783 Reichstein, M., Tenhunen, J., Rouspard, O., Ourcival, J. M., Rambal, S., Miglietta, F.,  
784 Peressotti, A., Pecchiari, M., Tirone, G. and Valentini, R.: Inverse modeling of  
785 seasonal drought effects on canopy CO<sub>2</sub>/H<sub>2</sub>O exchange in three Mediterranean  
786 ecosystems, *J. Geophys. Res.*, 108(23), 2003.

787 Reichstein, M., Falge, E., Baldocchi, D., Papale, D., Aubinet, M., Berbigier, P.,  
788 Bernhofer, C., Buchmann, N., Gilmanov, T., Granier, A., Grunwald, T.,  
789 Havranek, K., Ilvesniemi, H., Janous, D., Knohl, A., Laurila, T., Lohila,  
790 A., Loustau, D., Matteucci, G., Meyers, T., Miglietta, F., Ourcival, J. M.,  
791 Pumpanen, J., Rambal, S., Rotenberg, E., Sanz, M., Tenhunen, J., Seufert, G.,  
792 Vaccari, F., Vesala, T., Yakir, D. and Valentini, R.: On the separation of net  
793 ecosystem exchange into assimilation and ecosystem respiration: Review and  
794 improved algorithm, *Glob. Chang. Biol.*, 11(9), 1424–1439, 2005.

795 Sala, A. and Tenhunen, J. D.: Simulations of canopy net photosynthesis and  
796 transpiration in *Quercus ilex* L. under the influence of seasonal drought, *Agric. For.*  
797 *Meteorol.*, 78 203–222, 1996.

798 Sala, A., Woodruff, D. R. and Meinzer, F. C.: Carbon dynamics in trees: feast or  
799 famine?, *Tree Physiol.*, 32(6), 764–775, 2012.

800 Salzer, M. G., Hughes, M. K., Bunn, A. G. and Kipfmüller, K. F.: Recent  
801 unprecedented tree-ring growth in bristlecone pine at the highest elevations and  
802 possible causes., *PNAS*, 106(48), 20348–20353, 2009.

803 Saurer, M., Spahni, R., Frank, D.C., Joos, F., Leuenberger, M., Loader, N.J., McCarroll,  
804 D., Gagen, M., Poulter, B., Siegwolf, R. T. W., Andreu-Hayles, L., Boettger, T.,  
805 Dorado, I., Fairchild, I. J., Friedrich, M., Gutierrez, E., Haupt, M., Hiltunen, E.,  
806 Heinrich, I., Helle, G., Grud, H., Jalkanen, R., Levanič, T., Linderholm, H. W.,  
807 Robertson, I., Sonninen, E., Treydte, K., Waterhouse, J. S., Woodley, E. J., Wynn,  
808 P. M. and Young, G. H. F.: Spatial variability and temporal trends in water-use  
809 efficiency of European forests., *Glob. Chang. Biol.*, 3700–3712, 2014.

810 Schaefer, K., Schwalm, C.R., Williams, C., Arain, M.A., Barr, A., Chen, J.M., Davis,  
811 K. J., Dimitrov, D., Hilton, T.W., Hollinger, D.Y., Humphreys, E., Poulter, B.,  
812 Raczka, B.M., Richardson, A.D., Sahoo, A., Thornton, P., Vargas, R., Verbeeck,  
813 H., Anderson, R., Baker, I., Black, T.A., Bolstad, P., Chen, J., Curtis, P.S., Desai,  
814 A. R., Dietze, M., Dragoni, D., Gough, C., Grant, R. F., Gu, L., Jain, A., Kucharik,  
815 C., Law, B., Liu, S., Lokipitiya, E., Margolis, H.A., Matamala, R., McCaughey, J.  
816 H., Monson, R., Munger, J.W., Oechel, W., Peng, C., Price, D. T., Ricciuto, D.,  
817 Riley, W. J., Roulet, N., Tian, H., Tonitto, C., Torn, M., Weng, E. and Zhou, X.: A  
818 model-data comparison of gross primary productivity: Results from the North  
819 American Carbon Program site synthesis, *J. Geophys. Res.*, 117(G3), G03010,  
820 2012.

821 Simioni, G., Durand-Gillmann, M. and Huc, R.: Asymmetric competition increases leaf  
822 inclination effect on light absorption in mixed canopies, *Ann. For. Sci.*, 70(2), 123–  
823 131, 2013.

824 Sun, Y., Gu, L., Dickinson, R. E., Norby, R. J., Pallardy, S. G. and Hoffman, F. M.:  
825 Impact of mesophyll diffusion on estimated global land CO<sub>2</sub> fertilization, *Proc.*  
826 *Natl. Acad. Sci. U. S. A.*, 111(44), 15774–15779, 2014.

827 Tolwinski-Ward, S. E., Evans, M. N., Hughes, M. K. and Anchukaitis, K. J.: An  
828 efficient forward model of the climate controls on interannual variation in tree-ring  
829 width, *Clim. Dyn.*, 36(11-12), 2419–2439, 2011.

830 Touchan, R., Shishov, V. V., Meko, D. M., Nouiri, I. and Grachev, A.: Process based  
831 model sheds light on climate sensitivity of Mediterranean tree-ring width,  
832 *Biogeosciences*, 9(3), 965–972, 2012.

833 Vaganov, E.A., Hughes, M.K., Shashkin, A.V. *Growth Dynamics of Conifer Tree*  
834 *Rings: Images of Past and Future Environments*. Springer, New York. 2006.

835 Vaz, M., Pereira, J. S., Gazarini, L. C., David, T. S., David, J. S., Rodrigues, A.,  
836 Maroco, J. and Chaves, M. M.: Drought-induced photosynthetic inhibition and  
837 autumn recovery in two Mediterranean oak species (*Quercus ilex* and *Quercus*  
838 *suber*), *Tree Physiol.*, 30(8), 946–956, 2010.

839 Voltas, J., Camarero, J. J., Carulla, D., Aguilera, M., Ortiz, A. and Ferrio, J. P.: A  
840 retrospective, dual-isotope approach reveals individual predispositions to winter-  
841 drought induced tree dieback in the southernmost distribution limit of Scots pine.,  
842 *Plant. Cell Environ.*, 36(8), 1435–48, 2013.

843 **Table 1.** Characteristics of mean annual gross primary productivity, climatic (annual  
844 means) and growth data. Standard deviations are shown between parentheses.  
845 Precipitation=mean annual precipitation; Tmax=annual mean of mean daily maximum  
846 temperature; Tmin= annual mean of mean daily minimum temperature.  
847 Length=chronology year replicated with more than 5 radii; RW=mean annual ring-  
848 width; Rbs = mean correlation between series; AR = mean autocorrelation of raw series;  
849 MS = mean sensitivity; EPS = mean expressed population signal Rbs, AR, MS and EPS  
850 are classical statistics to characterise growth chronologies, and follow Fritts (1976).  
851

		Fontblanche		Puechabon
Flux Data	Period	2008-2012		2001-2013
	GPP annual (g C m <sup>-2</sup> year <sup>-1</sup> )	1431.4 (305.4)		1207.3 (206.7)
Climate	Period	1964-2012		1954-2013
	Precipitation (mm)	642.7 (169.7)		1002.6 (328.2)
	Tmax (°C)	20.6 (0.9)		17.8 (1.26)
	Tmin (°C)	8.8 (0.5)		8.1 (0.8)
Growth Data	Species	<i>P. halepensis</i>	<i>Q. ilex</i>	<i>Q. ilex</i>
	# Trees/Radii	25/47	15/30	17/32
	Length	1910-2013	1941-2013	1941-2005
	RW (mm)	2.19 (1.1)	1.25 (0.7)	1.13 (0.7)
	MS	0.308	0.372	0.443
	AR	0.684	0.591	0.436
	Rbs	0.541	0.281	0.457
	EPS	0.963	0.884	0.949

852



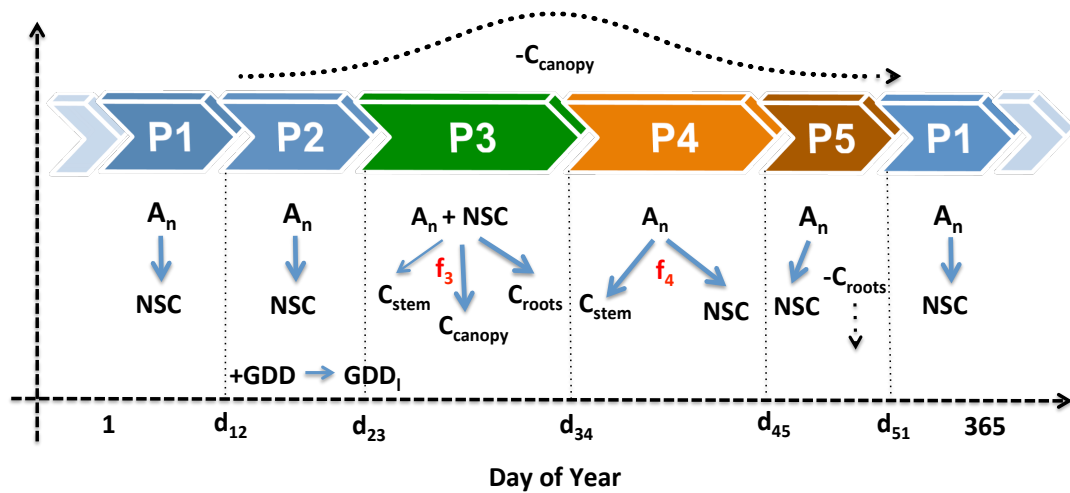
853 **Table 2.** Model parameters. Those parameter differing between sites were optimized  
854 either with GPP data (photosynthesis and allocation module) or with growth-based  
855 biomass increment chronologies (allocation module). The rest were common parameters  
856 for both sites and selected while developing the model in the first step for Fontblanche  
857 using GPP data (represented in ‘Cal’ with a ‘-‘). Meaning of parameters, equation  
858 number (E#) and phenophase [P#] are as in the text in Material and Methods.  
859 Fontb=Fontblanche; Puech=Puechabon; Cal=local parameters to be calibrated with GPP  
860 or stem biomass increment data (SBI).

861

Process	Process/Equation #	Parameter	Fontb	Puech	Units	Cal	
Photosynthesis	Leaf photosynthesis [E2]	$J_{coef}$	QUIL	1.59		$\mu\text{mol C m}^{-2} \text{s}^{-1}$	-
			PIHA	1.44	-		
	Leaf photosynthesis [E3]	$V_{max}$	QUIL	32.3		$\mu\text{mol C m}^{-2} \text{s}^{-1}$	-
			PIHA	46.0	-		
		$V_b$	QUIL	-0.106		$^{\circ}\text{C}^{-1}$	-
			PIHA	-0.180	-		
	$V_{ip}$	QUIL	13.7		$^{\circ}\text{C}$	-	
		PIHA	20.0	-			
	Stress $V_{cmax}$ [E4]	$p_{str}$	-0.05		$\text{mm}^{-1}$	-	
	Stomatal conductance [E5]	$g_l$	QUIL	7.5		-	-
PIHA			6.1	-			
Water stress [E6]	$VPD_0$	30000		Pa	-		
	$Soil_b$	-0.054		$\text{mm}^{-1}$	-		
	$Soil_{ip}$	22.2	81.8	mm	GPP		
Allocation	Respiration [E7]	$p_{respi}$	-0.225		$^{\circ}\text{C}^{-1}$	-	
	Stress LAI [E8]	$p_{LAI}$	65.5		mm	-	
	[P2]	$GDD_1$	203.3		$^{\circ}\text{C}$	-	
	Stored carbon buds [P3]	$C_{bud}$	7		$\text{g C day}^{-1}$	-	
	[P5]	Photoperiod	9.5		hours	-	
	Allocation canopy [P3], [E9]	$st_{4moist}$	-0.089	-0.173	$\text{mm}^{-1}$	GPP	
		$st_{4temp}$	53.3	75	$^{\circ}\text{C}$	GPP	
		$st_{4sd}$	26.9	26.1	$^{\circ}\text{C}$	GPP	
	Allocation stem [P3], [E10]	$st_{3moist}$	-0.045	-0.117	$\text{mm}^{-1}$	SBI	
		$st_{3temp}$	32.9	6.3	$^{\circ}\text{C}$	SBI	
$st_{3sd}$		38.0	3.0	$^{\circ}\text{C}$	SBI		
Allocation stor/stem [P4], [E11]	$st_{4moist}$	200.8	119.3	mm	SBI		
	$st_{4temp}$	0.060	-0.097	$^{\circ}\text{C}^{-1}$	SBI		

862

863 **Figure 1.** Outline of the different phenological phases (P1 to P5) and carbon allocation  
864 in the model within a given year.  $A_n$ =net daily carbon assimilation; NSC=storage (non-  
865 structural carbohydrates); GDD=growing degree days,  $GDD_I$ =parameter determining  
866 shift from P2 to P3 (see text);  $C$ =carbon allocated either to the stem, canopy or roots;  
867  $d$ =day of year. Solid arrows correspond to allocation within the plant whereas dashed  
868 arrows to correspond to litterfall (canopy or roots).  $f_3$  and  $f_4$  are nonlinear functions of  
869 soil water content and temperature determining carbon allocation to different  
870 compartments (see text for more details).  
871



872 **Figure 2.** Growth (basal area increment, BAI,  $\text{cm}^2 \cdot \text{year}^{-1}$ ) and biomass allocated to the  
 873 tree stem ( $\text{g C} \cdot \text{m}^{-2} \cdot \text{year}^{-1}$ ) of *Q. ilex* and *P. halepensis* at Fontblanche (growth shown in  
 874 (a), biomass in (b)) and *Q. ilex* at Puechabon (growth and stem biomass shown in (c)).  
 875 A vertical dashed line marks the release event in Fontblanche produced by the enhanced  
 876 winter mortality in 1985 in (a). Dark lines for BAI correspond to yearly means while  
 877 grey polygons show confidence intervals (at 95%) on the standard errors of the mean.

878

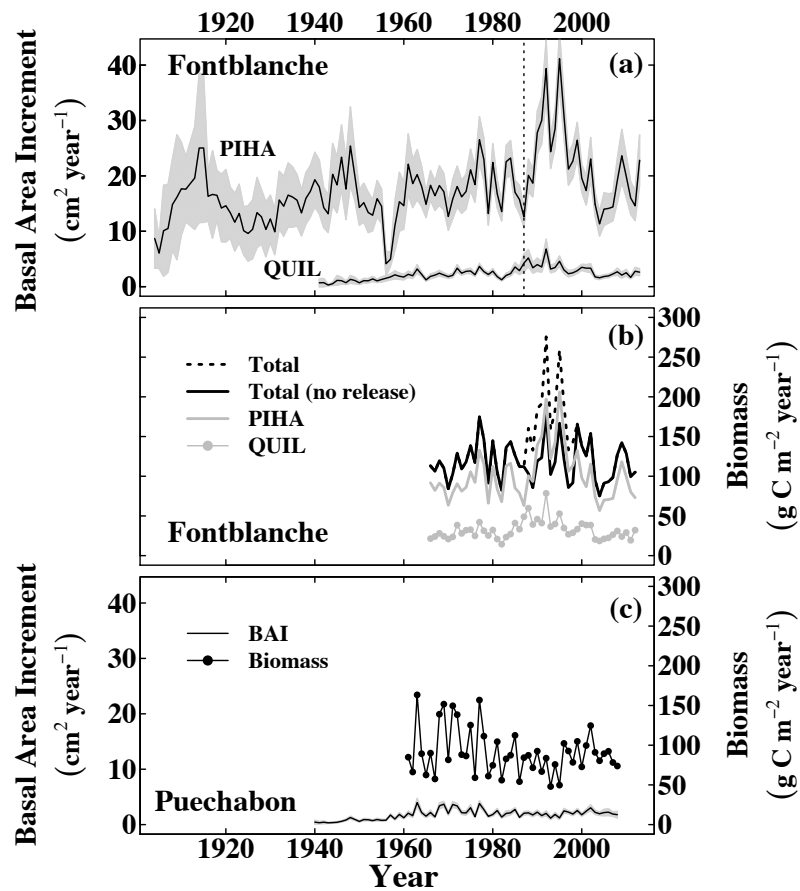


**Figure 3.** Daily gross primary productivity (GPP) at Puechabon (2001-2013, black dots, blue line) and Fontblanche (2008-2012, orange dots, red line). DOY=day of year. Thick lines correspond to smoothers fitted to the mean to highlight seasonal trends at the two sites.

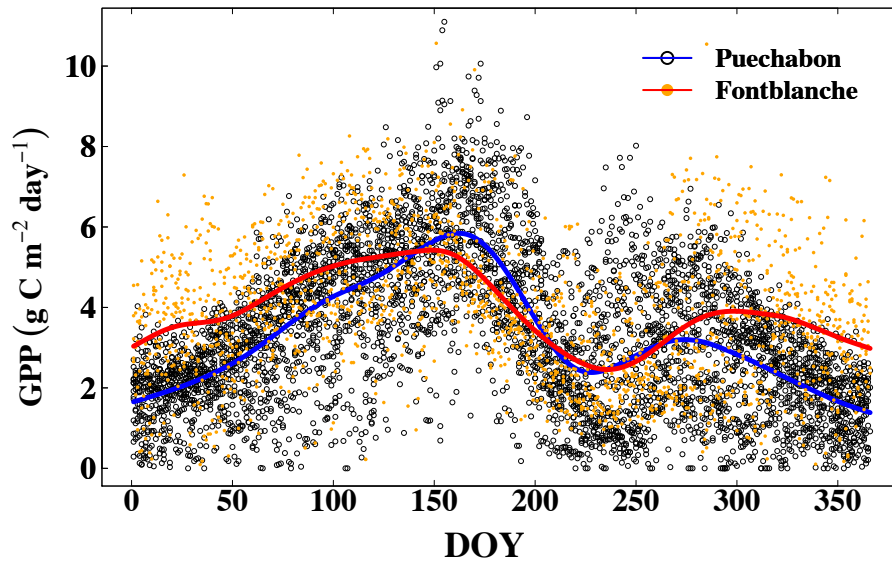


**Figure 4.** Model fit to stem biomass increment (a) and GPP (b) in Fontblanche; and stem biomass increment (c) and GPP (d) in Puechabon.  $R^2$ =coefficient of determination;  $\rho$ =linear correlation between estimated and observed data,  $\rho_{low15}$ =linear correlation between estimated and observed data smoothed with a 15 year low-pass filter (blue and red lines in (b) and (c)). Polygons behind the estimated values in (a) and (c) correspond to confidence intervals of the mean: solid grey polygons for estimated values and dashed polygons for observed stem biomass increment values.

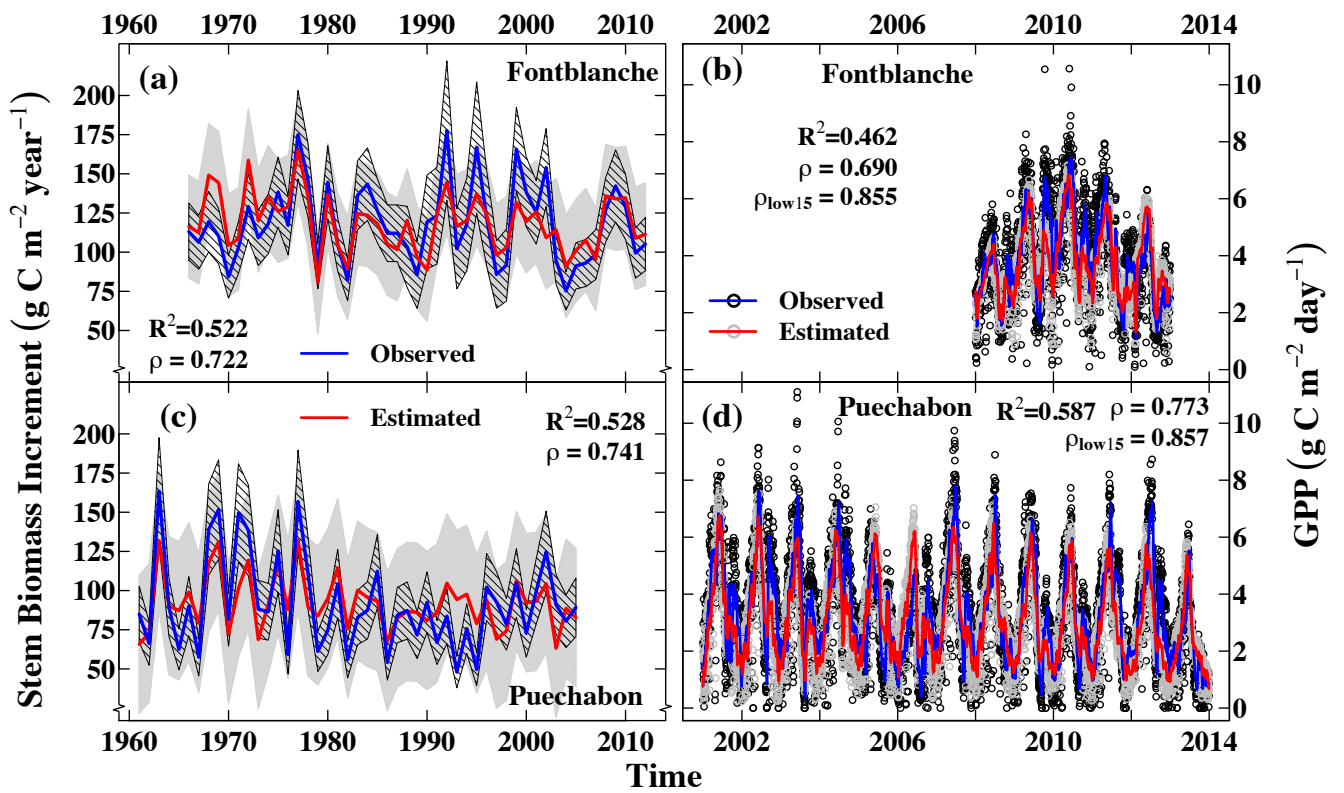


**Figure 5.** Modelled carbon allocation trajectory to the stem when leaf flush has finished in phenological period [P4]. We show the unitless modifier  $1-h_4(i)$  (i.e.  $h_4(i)$  is the portion of allocated carbon to storage) from  $C_{stem}(i) = A_N(i) \cdot [(1-h_4(i))]$  as from [E11]. The modifier  $[0,1]$  is a function of soil water content (SWC) and maximum temperature ( $T_{max}$ ) and multiplies available daily carbon to distribute daily carbon allocated between secondary growth and storage.

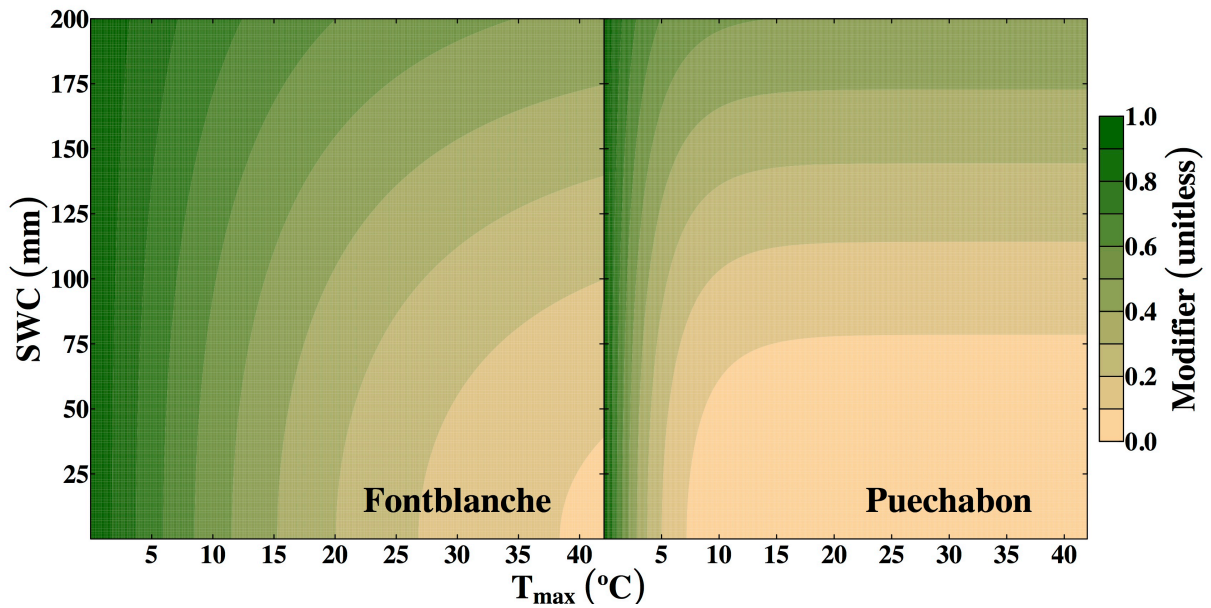


**Figure 6.** Modelled total annual stand gross primary productivity (GPP) and mean stomatal conductance of sunny leaves ( $g_s$ ) for Fontblanche (a) and Puechabon (b) for the period where meteorological data were available.

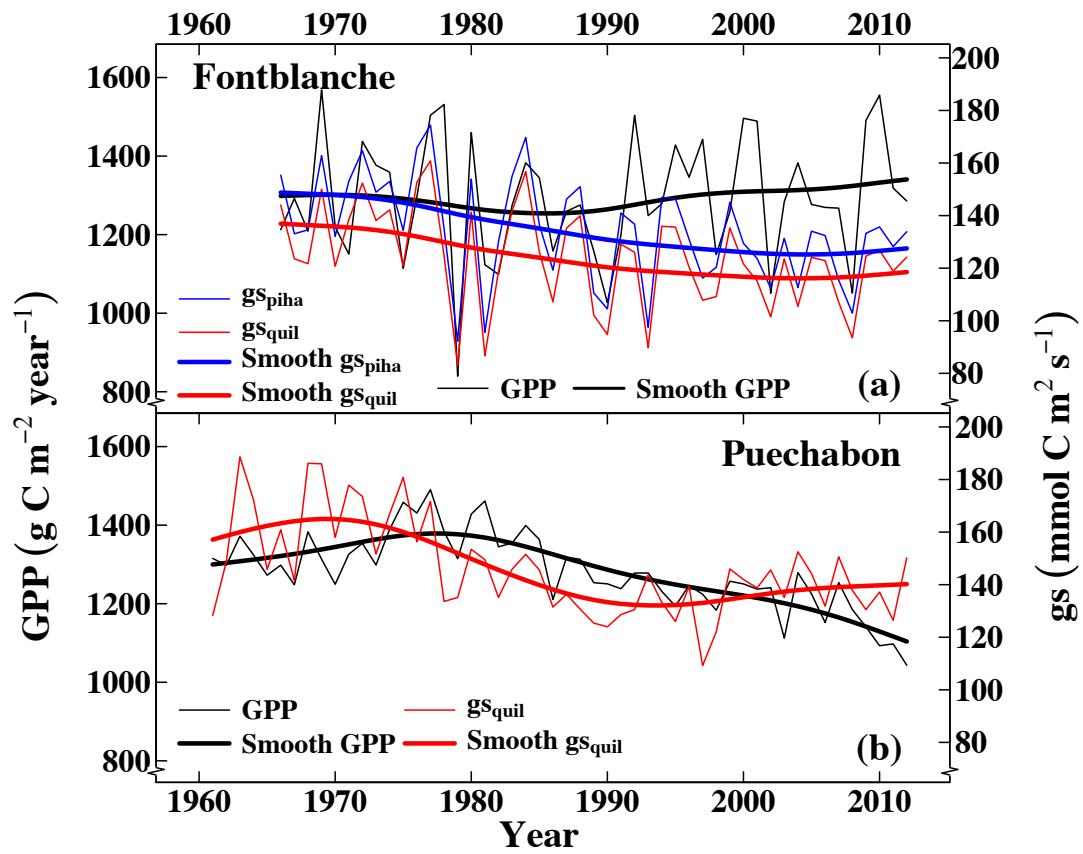


**Figure 7.** Ecosystem WUE (integral annual) and iWUE for sun leaves (mean daily, for PIHA and QUIL separated in Fontblanche) for (a) Fontblanche and (b) Puechabon for the period where we had available meteorological data.

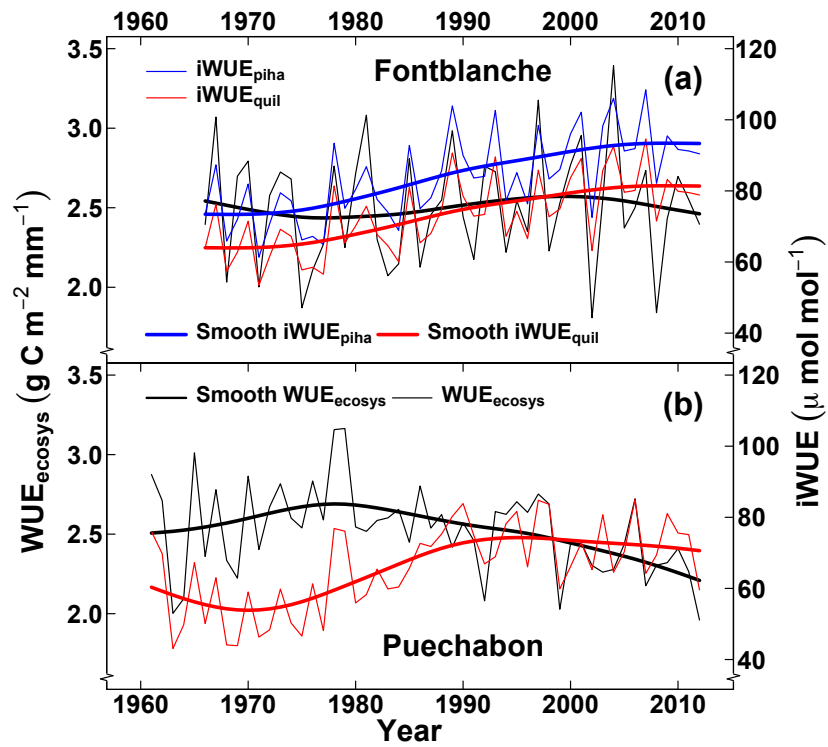




**Figure A1.** Mean climatic time series in the last 50 years. (a) annual precipitation; (b) and (c) annual maximum ( $T_{max}$ ) and minimum ( $T_{min}$ ) temperatures for Fontblanche (b) and Puechabon (c).

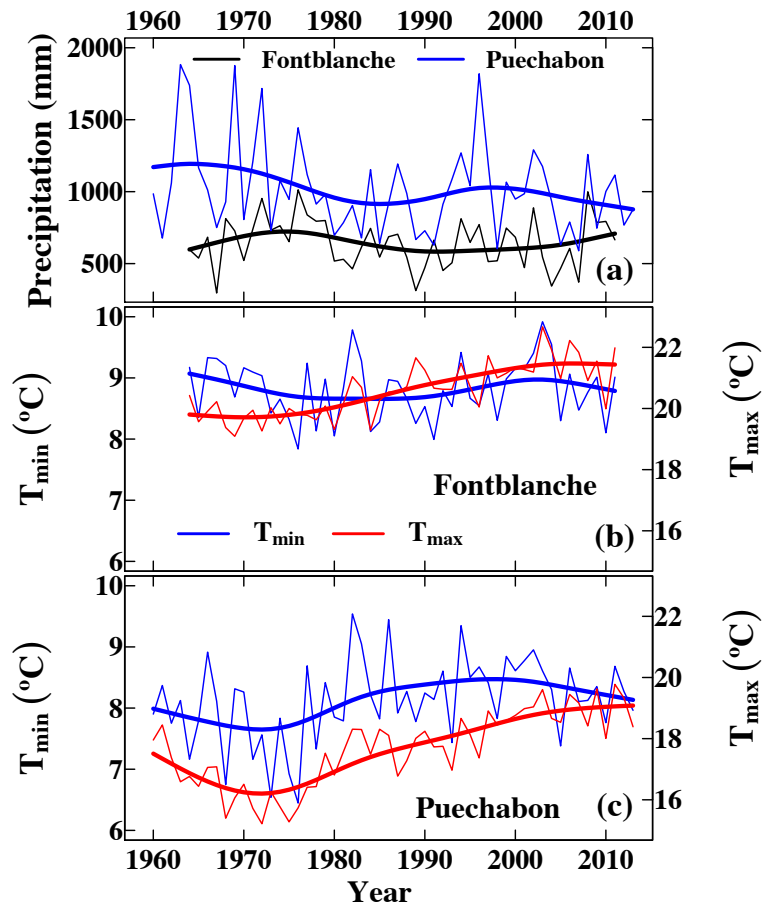


**Figure A2.** Diameter (dbh, cm) and age (years) distribution of trees included in the chronologies. Frequencies are calculated separately by species and site.

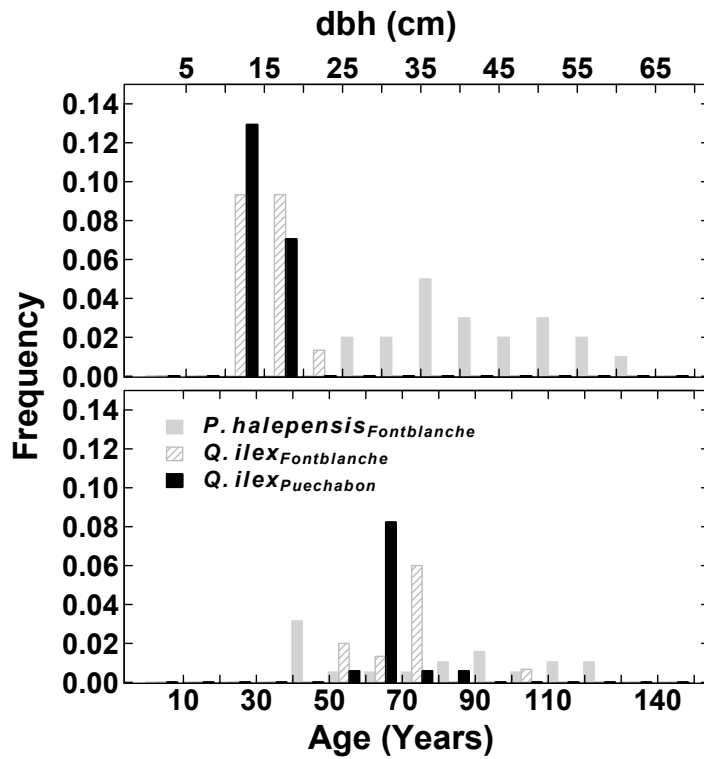


**Figure A3.** Simulated maximum annual leaf area index LAI ( $\text{m}^2 \cdot \text{m}^{-2}$ ) and total annual stand transpiration E ( $\text{mm}/\text{year}$ ) in Fontblanche (a) and Puechabon (b).

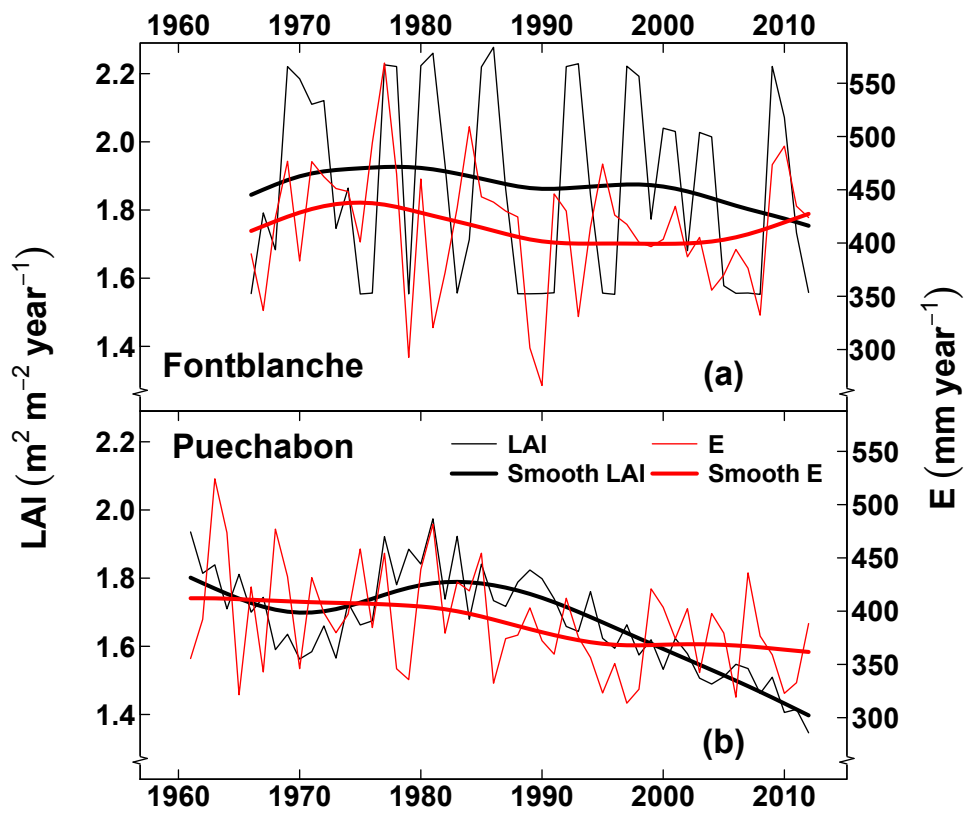


**Figure A4.** Simulated mean annual stomatal conductance ( $g_s$ ) as a function of mean  $[\text{CO}_2]$  (a) and mean maximum temperature (b).

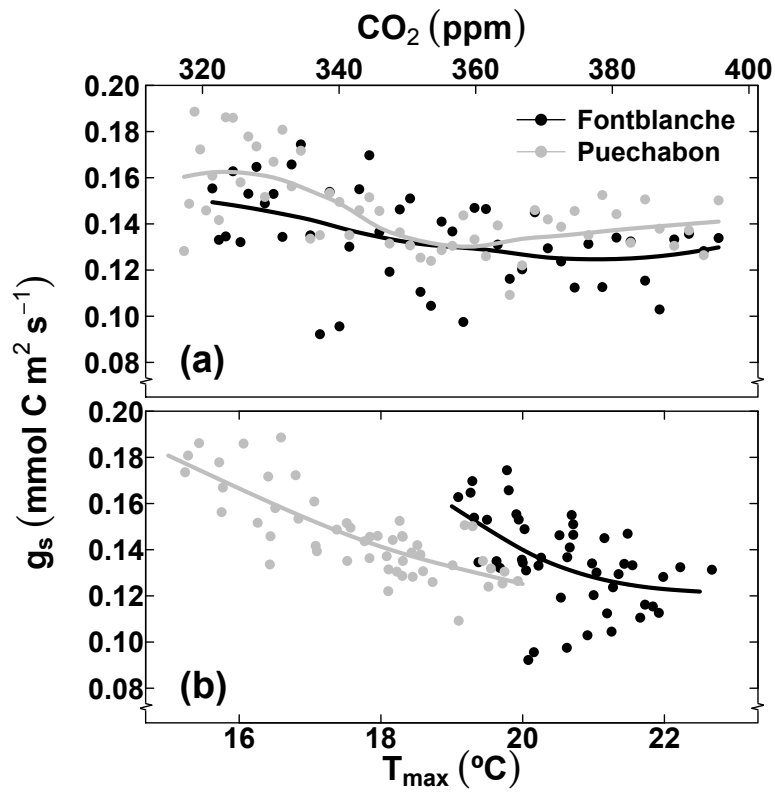


**Figure A5.** Simulated non-structural carbohydrate content (NSC) in the storage pool at both sites. The period 1995-2012 is shown to highlight within year variability.

